

A *para*-Hydrogen Investigation of Palladium-Catalyzed Alkyne Hydrogenation

Joaquín López-Serrano,[†] Simon B. Duckett,^{*,†} Stuart Aiken,[†]
Karina Q. Almeida Leñero,[‡] Eite Drent,[‡] John P. Dunne,[†] Denis Konya,[†] and
Adrian C. Whitwood[†]

Contribution from the Department of Chemistry, University of York, Heslington, York, U.K.
YO10 5DD, and Shell Research & Technology Centre Amsterdam, Badhuisweg 3,
NL-1031 CM. Amsterdam, Netherlands

Received January 16, 2007; E-mail: sbd3@york.ac.uk

Abstract: The complexes [Pd(bcope)(OTf)₂] (**1a**), where bcope is (C₈H₁₄)PCH₂–CH₂P(C₈H₁₄), and [Pd('bucope)(OTf)₂] (**1b**), where 'bucope is (C₈H₁₄)PC₆H₄CH₂P('Bu)₂, catalyze the conversion of diphenylacetylene to *cis*- and *trans*-stilbene and 1,2-diphenylethane. When this reaction was studied with *para*-hydrogen, the characterization of [Pd(bcope)(CHPhCH₂Ph)](OTf) (**2a**) and [Pd('bucope)(CHPhCH₂Ph)](OTf) (**2b**) was achieved. Magnetization transfer from the α -H of the CHPhCH₂Ph ligands in these species proceeds into *trans*-stilbene. This process has a rate constant of 0.53 s⁻¹ at 300 K in methanol-*d*₄ for **2a**, where $\Delta H^\ddagger = 42 \pm 9$ kJ mol⁻¹ and $\Delta S^\ddagger = -107 \pm 31$ J mol⁻¹ K⁻¹, but in CD₂Cl₂ the corresponding rate constant is 0.18 s⁻¹, with $\Delta H^\ddagger = 79 \pm 7$ kJ mol⁻¹ and $\Delta S^\ddagger = 5 \pm 24$ J mol⁻¹ K⁻¹. The analogous process for **2b** was too fast to monitor in methanol, but in CD₂Cl₂ the rate constant for *trans*-stilbene formation is 1.04 s⁻¹ at 300 K, with $\Delta H^\ddagger = 94 \pm 6$ kJ mol⁻¹ and $\Delta S^\ddagger = 69 \pm 22$ J mol⁻¹ K⁻¹. Magnetization transfer from one of the two inequivalent β -H sites of the CHPhCH₂Ph moiety proceeds into *trans*-stilbene, while the other site shows transfer into H₂ or, to a lesser extent, *cis*-stilbene in CD₂Cl₂, but in methanol it proceeds into the vinyl cations [Pd(bcope)(CPh=CHPh)(MeOD)](OTf) (**3a**) and [Pd('bucope)(CPh=CHPh)(MeOD)](OTf) (**3b**). When the same magnetization transfer processes are monitored for **1a** in methanol-*d*₄ containing 5 μ L of pyridine, transfer into *trans*-stilbene is observed for two sites of the alkyl, but the third proton now becomes a hydride ligand in [Pd(bcope)(H)(pyridine)](OTf) (**5a**) or a vinyl proton in [Pd(bcope)(CPh=CHPh)(pyridine)](OTf) (**4a**). For **1b**, under the same conditions, two isomers of [Pd('bucope)(H)(pyridine)](OTf) (**5b** and **5b'**) and the neutral dihydride [Pd('bucope)(H)₂] (**7**) are detected. The single vinylic CH proton in **3** and the hydride ligands in **4** and **5** appear as strong emission signals in the corresponding ¹H NMR spectra.

Introduction

The metal-catalyzed reduction of unsaturated hydrocarbons has received much attention in the past because of the vast number of opportunities that exist to prepare high-value products. Such reactions therefore feature in many multistep syntheses. For instance, the hydroformylation of an alkene is an industrially important reaction of great significance that produces detergents and plasticizer alcohols.¹ The closely related methoxycarbonylation of ethene to form methyl propanoate, an intermediate in the manufacture of methyl methacrylate, is another well-studied example where the reduction of a double bond by a metal catalyst (e.g., Pd) is required.² Less attention has been focused, however, on the hydrogenation of triple bonds. Earlier investigations of alkyne hydrogenation led to the development of heterogeneous catalysts such as the Lindlar

catalyst.^{3,4} More recently, a comprehensive study on the selective semihydrogenation of alkynes to (*Z*)-alkenes by homogeneous α -diiminepalladium(0) catalysts has been carried out by Elsevier et al.^{5–7} A palladium hydride, or more generally a metal hydride, is often proposed to have a role in such reactions,^{1,8} although the direct detection of such species is relatively rare.⁹ Recently, [(1,2-(CH₂P–'Bu)₂C₆H₄)Pd(H)(MeOH)], a key intermediate in the methoxycarbonylation of alkenes, was detected by NMR spectroscopy,¹⁰ and further investigations afforded the identification of the related alkyl species [(1,2-(CH₂P–'Bu)₂C₆H₄)Pd(CH₂CH₃)]⁺, which features a β -H agostic interaction. This

[†] University of York.

[‡] Shell Research & Technology Centre Amsterdam.

- (1) Konya, D.; Almeida Leñero, K. Q.; Drent, E. *Organometallics* **2006**, *25*, 3166–3174.
- (2) Clegg, W.; Eastham, G. R.; Elsegood, M. R. J.; Heaton, B. T.; Iggo, J. A.; Tooze, R. P.; Whyman, R.; Zacchini, S. *Organometallics* **2002**, *21*, 1832–1840.

- (3) Lindlar, H. *Helv. Chim. Acta* **1952**, *35*, 446.
- (4) Lindlar, H.; Dubuis, R. *Org. Synth.* **1966**, *46*, 89.
- (5) Dedieu, A.; Humbel, S.; Elsevier, C.; Grauffel, C. *Theor. Chem. Acc.* **2004**, *112*, 305–312.
- (6) Kluwer, A. M.; Koblenz, T. S.; Jonischkeit, T.; Woelk, K.; Elsevier, C. J. *J. Am. Chem. Soc.* **2005**, *127*, 15470–15480.
- (7) van Laren, M. W.; Duin, M. A.; Klerk, C.; Naglia, M.; Rogolino, D.; Pelagatti, P.; Bacchi, A.; Pelizzi, C.; Elsevier, C. J. *Organometallics* **2002**, *21*, 1546–1553.
- (8) del Río, I.; Claver, C.; van Leeuwen, P. W. N. M. *Eur. J. Inorg. Chem.* **2001**, 2719–2738.
- (9) Grushin, V. V. *Chem. Rev.* **1996**, *96*, 2011–2033.
- (10) Clegg, W.; Eastham, G. R.; Elsegood, M. R. J.; Heaton, B. T.; Iggo, J. A.; Tooze, R. P.; Whyman, R.; Zacchini, S. *Dalton Trans.* **2002**, 3300–3308.

species is proposed to be in equilibrium with the alkene hydride $[(1,2-(\text{CH}_2\text{P}-\text{tBu}_2)_2\text{C}_6\text{H}_4)\text{Pd}(\text{H})(\eta^2\text{-CH}_2=\text{CH}_2)]^+$.² However, the detection of such species alone does not necessarily imply that they take an active part in catalysis. Truly catalytic species should have a dynamic existence under the reaction conditions and must react further with other reagents during catalysis. Consequently, their concentration at equilibrium is normally very low.

It has been shown that *para*-hydrogen-induced polarization (PHIP) can be used to enable the direct NMR detection of many metal hydride signals for complexes in solution that would otherwise be invisible. This approach therefore overcomes the inherent low sensitivity of NMR spectroscopy and makes it applicable to the study of catalytic reactions.^{11–15} Insensitive heteronuclei like ^{13}C and ^{31}P , which are scalar-coupled to the enhanced hydride signals, can also be detected indirectly via appropriate one-dimensional^{16,17} and two-dimensional^{18–22} cross polarization experiments. PHIP NMR spectroscopy has also been shown to permit the direct identification of metal complexes without the need for enhancement of metal hydride signals, an example being the characterization of intermediates in cobalt-catalyzed hydroformylation through proton resonances of ancillary acyl ligands.²³ In a preliminary study, we reported the detection of an alkylpalladium complex that was shown to be a key intermediate in the palladium-catalyzed alkyne hydrogenation of diphenylacetylene.²⁴ The three alkyl protons and the two carbons of the CHCH_2 backbone of the alkyl ligand were unambiguously assigned by PHIP NMR spectroscopy. The minimal structure of this species was therefore confirmed to be $\text{Pd}(\text{bcope})(\text{PhCHCH}_2)$. Subsequent studies using $\text{Pd}(\text{PEt}_3)_2(\text{OTf})_2$ as the metal precursor extended this study further and enabled the detection of related vinyl hydride species.²⁵

Two possible mechanisms were considered to account for these observations. One, a cationic mechanism, starts with a palladium monohydride cation. Subsequent coordination and migratory insertion of the alkyne leads to a vinyl complex, from which the alkene is released after dihydrogen addition (Figure 1). The second proposed mechanism (Figure 2), a neutral cycle, requires controlled reduction of a $\text{Pd}(\text{II})$ triflate to a $\text{Pd}(\text{0})$ bisphosphine complex. Reduction of $\text{Pd}(\text{II})$ precursors to $\text{Pd}(\text{0})$ species is accepted as the starting point of many catalytic

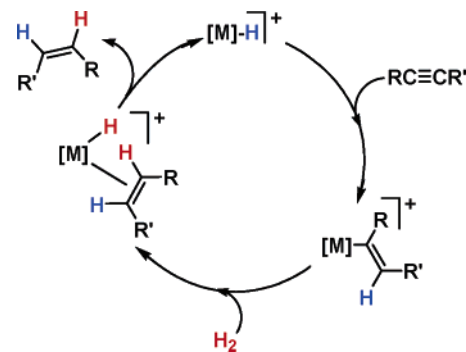


Figure 1. Schematic cationic mechanism for palladium bisphosphine $[\text{M}]$ -catalyzed alkyne hydrogenation.

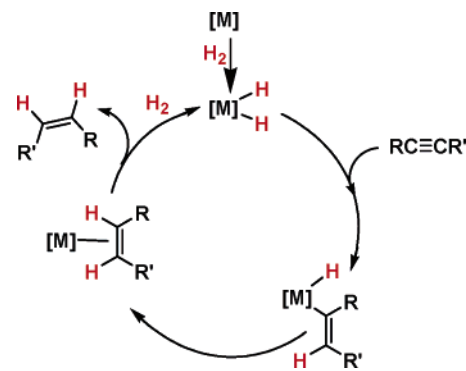


Figure 2. Schematic neutral mechanism for palladium bisphosphine $[\text{M}]$ -catalyzed alkyne hydrogenation.

reactions,^{26,27} and a mechanism for this reaction based on $\text{Pd}(\text{0})$ species has been recently proposed.^{5,6} Our initial mechanistic proposal for the *bcope* hydrogenation system followed the neutral cycle and was supported by a preliminary theoretical study (DFT). The proposed reaction cycle also met the key constraints imposed by PHIP NMR spectroscopy.^{20,21}

Herein we describe new experimental evidence for the generation of monohydride precursors which, in conjunction with an extensive PHIP NMR study, strongly suggests that a cationic mechanism is preferred for the hydrogenation of alkynes catalyzed by palladium(II) bisphosphine triflates.

Experimental Section

General Conditions. All manipulations were carried out under inert atmosphere conditions, using standard Schlenk techniques (with vacuum of up to 10^{-2} mbar, with N_2 or Ar as an inert atmosphere) or high-vacuum techniques (10^{-4} mbar). Dry N_2 and Ar were purchased from BOC Gases. Storage and manipulation of samples was carried out using standard glovebox techniques, under an atmosphere of N_2 , using an Alvic Scientific Gas Shield glovebox equipped with a freezer (-32°C), vacuum pump, and N_2 purge facilities. Solvents were obtained as analytical grade from Fisher. Diethyl ether was dried by refluxing under nitrogen over sodium wire, while dichloromethane and methanol were dried over calcium hydride. The deuterated solvents methanol- d_4 and CD_2Cl_2 were purchased from Aldrich and stored under N_2 but used without further purification (when dried solvents were employed, no difference in the speciation was observed in the reactions described in this paper). $\text{Pd}(\text{PhCN})_2\text{Cl}_2$ was prepared as described in the literature (PdCl_2 was purchased from Johnson Matthey and PhCN from Lancaster). AgOTf was obtained from Aldrich and used as received. NMR spectra were obtained on a Bruker DRX 400, DSX

- (11) Bowers, C. R.; Weitekamp, D. P. *Phys. Rev. Lett.* **1986**, *57*, 2645–2648.
- (12) Natterer, J.; Bargon, J. *Nucl. Magn. Reson. Spectrosc.* **1997**, *31*, 293–315.
- (13) Duckett, S. B.; Sleight, C. J. *Prog. Nucl. Magn. Reson. Spectrosc.* **1999**, *34*, 71–93.
- (14) Duckett, S. B.; Blazina, D. *Eur. J. Inorg. Chem.* **2003**, *16*, 2901–2912.
- (15) Blazina, D.; Duckett, S. B.; Dunne, J. P.; Godard, C. *Dalton Trans.* **2004**, *17*, 2601–2609.
- (16) Duckett, S. B.; Newell, C. L.; Eisemberg, R. *J. Am. Chem. Soc.* **1993**, *115*, 1156–1157.
- (17) Haake, M.; Natterer, J.; Bargon, J. *J. Am. Chem. Soc.* **1996**, *118*, 8688–8691.
- (18) Duckett, S. B.; Barlow, G. K.; Partridge, M. G.; Messerle, B. A. *Dalton Trans.* **1995**, 3427–3430.
- (19) Duckett, S. B.; Mawby, R. J.; Partridge, M. G. *Chem. Commun.* **1996**, 383–384.
- (20) Jang, M.; Duckett, S. B.; Eisemberg, R. *Organometallics* **1996**, *15*, 2863–2865.
- (21) Millar, S. P.; Jang, M.; Lachicotte, R. J.; Eisemberg, R. *Inorg. Chim. Acta* **1998**, *270*, 363–375.
- (22) Messerle, B. A.; Sleight, C. J.; Partridge, M. G.; Duckett, S. B. *Dalton Trans.* **1999**, 1429–1435.
- (23) Godard, C.; Duckett, S. B.; Polas, S.; Tooze, R. P.; Whitwood, A. C. *J. Am. Chem. Soc.* **2005**, *127*, 4994–4995.
- (24) Dunne, J. P.; Aiken, S.; Duckett, S. B.; Konya, D.; Lenner, K. Q. A.; Drent, E. *J. Am. Chem. Soc.* **2004**, *126*, 16708–16709.
- (25) López-Serrano, J.; Duckett, S. B.; Lledós, A. *J. Am. Chem. Soc.* **2006**, *128*, 9596–9597.

- (26) Streiter, E. R.; Blackmond, D. G.; Buchwald, S. L. *J. Am. Chem. Soc.* **2003**, *125*, 13978–13980.
- (27) Amatore, C.; Jutand, A. *Acc. Chem. Res.* **2000**, *33*, 314–321.

600, or DSX 700 spectrometer. For the hydrogenation studies, solutions of the palladium catalyst (ca. 5 mM; ca. 2.5 mg of catalyst in 500 μ L of deuterated solvent) in Young's tap NMR tubes were added to a ca. 40-fold excess of diphenylacetylene- d_{10} (ca. 20 mg; ca. 0.22 M) and then reacted with p -H₂ (3–3.5 atm). GC/MS data were collected on a Saturn 2000 gas chromatograph–mass spectrometer combination. A Factor-Form VF-6mg capillary column (30 m \times 0.25 mm i.d. and 0.25 μ m film thickness) was used for the GC separation. The initial oven temperature was 100 $^{\circ}$ C, and two temperature ramps (100–145 $^{\circ}$ C, 2.5 $^{\circ}$ C/min; 145–250 $^{\circ}$ C, 30 $^{\circ}$ C/min) were employed, with the final temperature being retained for 50 min. The helium carrier gas flow rate was 1.0 mL/min. Mass spectra were recorded in the electron ionization (EI) mode (70 eV, scanning the 30–650 m/z range). For the GC/MS measurements, dichloromethane or methanol solutions (1 mL) of the palladium complex (ca. 2 mg) and diphenylacetylene (ca. 50-fold excess, 22 mg) were degassed and placed under a H₂ atmosphere (4 atm). The mixtures were heated to 37 $^{\circ}$ C for 1 h, and the sample was shaken every 15 min. In order to obtain the product proportions, a series of relative response factors were produced for the different species via a control sample containing diphenylacetylene (9.3 mg, 98% purity), *cis*-stilbene (10 μ L, 10.14 mg, 97% purity), *trans*-stilbene (11.3 mg, 96% purity), and 1,2-diphenylethane (8.9 mg) in CH₂Cl₂ (5 mL). The bcope [(C₈H₁₄)PCH₂–CH₂P(C₈H₁₄)] and 'bucope [(C₈H₁₄)PC₆H₄–CH₂P('Bu)₂] ligands used in this work were prepared at Shell and the University of Bristol.^{28,29}

Synthesis of the Complexes. The triflate complexes used in this study were synthesized from their chloride analogues, which were prepared according to literature procedures.³⁰

Synthesis of [Pd(bcope)(OTf)₂] (1a). Pd(bcope)(Cl)₂ (120 mg, 0.25 mmol) was suspended in dry, degassed dichloromethane (30 mL) and AgOTf (158 mg, 0.65 mmol) added to the suspension. The mixture was stirred overnight in the absence of light. The new suspension was filtered off and the yellow solution concentrated to ca. 1 mL before *n*-hexane was added to precipitate the product, which was dried under vacuum. Yield: 121 mg or 63%. ³¹P{¹H} NMR (161 MHz, CD₂Cl₂): δ 73.11 (s). Anal. Calcd for C₂₀H₃₂Cl₂F₆O₆P₂S₂·2.5H₂O: C, 31.99; H, 4.83; S, 8.54. Found: C, 31.54; H, 4.94; S, 8.54.

Synthesis of [Pd('bucope)(OTf)₂]·5H₂O (1b). AgOTf (320 mg, 1.25 mmol) was added to a CH₂Cl₂ (10 mL) solution of [Pd('bucope)(Cl)₂] (200 mg, 0.31 mmol). The reaction mixture was stirred at room temperature for 72 h in the absence of light. The resulting suspension was filtered, and then the filtrate was evaporated to produce a colorless powder. Yield: 158 mg or 59%. ¹H NMR (400 MHz, CD₂Cl₂): δ 7.86–7.79 (m, 1 H, CHC₆H₄), 7.68–7.58 (m, 2 H, C₆H₄), 7.54–7.48 (m, 1 H, C₆H₄), 3.49 (m, 1 H, CH₂P), 3.35 (broad m, 1 H, C₈), 3.29 (apparent dd, $J_{\text{HH}} = 15.5$ Hz, $J_{\text{HP}} = 4.5$ Hz, 1 H, CH₂P), 2.97–2.61 (several m, 4 H, C₈), 2.34–1.34 (several m, 9 H, C₈), 1.56 (d, $J_{\text{HC}} = 15.5$ Hz, C'Bu), 1.22 (d, $J_{\text{HC}} = 15.5$ Hz, C'Bu). ¹³C{¹H} NMR (100 MHz, CD₂Cl₂): δ 137.75 (c, CCH₂PPh₂), 133.29 (s, CH C₆H₄), 132.96 (s, C₆H₄), 132.65 (s, C₆H₄), 129.39 (s, C₆H₄), 123.50 (c, CP), 41.63 (s, C'Bu), 40.53 (d, $J_{\text{CP}} = 16.0$ Hz, C'Bu), 29.85 (s, C'Bu), 29.10 (s, C'Bu), 24.52 (s, CH₂P). ³¹P{¹H} NMR (161 MHz, CD₂Cl₂): δ 110.0 (d, $J_{\text{PP}} = 7.2$ Hz, P'Bu), 31.13 (broad s, PC₈H₁₄). Anal. Calcd for C₂₅H₃₈F₆O₆P₂·PdS₂·5H₂O: C, 34.47; H, 5.55; S, 7.36. Found: C, 34.34; H, 5.22; S, 7.65.

In order to prepare the diphenylacetylene- I -¹³C- d_{10} used in this study, the following procedures were followed. First, *N,N*-dibutylbenzamide- I -¹³C- d_5 was prepared. To do this, a mixture of bromobenzene- d_5 (4 g, 24.7 mmol), dibutylamine (10 mL), ethyldiisopropylamine (10 mL), triphenylphosphine (520 mg, 8 mol %), bisbenzothiazolecarbene-palladium diiodide (650 mg, 4 mol %), and tetrabutylammonium bromide (4.5 g) in dimethylamine (30 mL) was degassed and heated

at 130 $^{\circ}$ C under 540 mmHg of ¹³CO for 5 h. The resulting mixture was cooled, diluted with HCl (1 M, 200 mL), and extracted with diethyl ether (3 \times 50 mL). The combined ethereal extracts were washed with water (100 mL) and dried (MgSO₄), and the solvent was removed under reduced pressure. The residue was chromatographed on silica using ethyl acetate (10% in hexanes), and the second band was collected to give *N,N*-dibutylbenzamide- I -¹³C- d_5 (3.16 g, 53%) as a pale orange oil. ¹H NMR (300 MHz, CDCl₃): δ 3.29 (bs, 2 H) 2.99 (bs, 2 H), 1.6–0.5 (m, 14 H). ¹³C NMR (75.45 MHz, CDCl₃): δ 172.160 (¹³CO), 137.43 (d, 65 Hz), 129.45, 128.22, 126.47, 49.19, 44.91, 31.21, 30.06, 20.17, 19.56, 14.38, 14.06. MS (EI): m/z 239 (M⁺, 12%) and 111 (M⁺ – Bu₂N, 100%).

Next acetophenone- I -¹³C- d_5 was synthesized. For this, methylolithium (1.6 M, 9.6 mL, 15 mm in Et₂O) was added to a solution of *N,N*-dibutylbenzamide- I -¹³C- d_5 (3 g, 12.8 mmol) in THF (30 mL) at room temperature under N₂. The solution was stirred at room temperature for 2 h, and then HCl (50 mL, 2 M) was added. The solution was extracted with dichloromethane (3 \times 50 mL), the organic extracts were washed with water (50 mL) and dried (MgSO₄), and the solvent was removed under reduced pressure. The residue was chromatographed on silica using ethyl acetate (10% in hexanes) to give acetophenone- I -¹³C- d_5 (1.33 g, 86%) as a pale yellow oil. ¹H NMR (300 MHz, CDCl₃): δ 2.32 (d, 3 H, $J = 8$ Hz). ¹³C NMR (75.45 MHz, CDCl₃): δ 195.94 (¹³CO), 135.72, 131.12, 128–126 (m), 24.98.

The acetophenone- I -¹³C- d_5 was then converted to 2-phenylacetophenone- I -¹³C- d_{10} . Palladium acetate (22 mg, 1 mol %), Pd₂(dba)₃ (48 mg, 1 mol %), and P'Bu₃ (64 μ L, 2 mol %) were dissolved in THF (20 mL) under N₂ and stirred for 10 min. Sodium *tert*-butoxide (2.09 g, 22 mmol) was added, followed by a solution of acetophenone- I -¹³C- d_5 (1.33 g, 10.5 mmol) and bromobenzene- d_5 (1.60 g, 9.9 mmol) in THF (20 mL). The resulting mixture was heated at 60 $^{\circ}$ C for 4 h, poured into HCl (50 mL, 1 M), and extracted with dichloromethane (3 \times 30 mL). The combined organic extracts were washed with water (50 mL) and dried (MgSO₄), and the solvent was removed under reduced pressure. The residue was used without further purification in the next step, the preparation of diphenylacetylene- I -¹³C- d_{10} .

A solution of PCl₅ (8.2 g, 39 mmol) and 2-phenylacetophenone- I -¹³C- d_{10} in benzene (30 mL) was heated at reflux for 3 h, cooled, poured into water (50 mL), and extracted with dichloromethane (3 \times 50 mL). The combined organic extracts were washed with water (50 mL) and dried (MgSO₄), and the solvent was removed under reduced pressure. The residue was dissolved in ethanolic NaOEt, heated at reflux for 4 h, cooled, poured into water (100 mL), and extracted with dichloromethane (3 \times 50 mL). The combined organic extracts were washed with water (50 mL) and dried (MgSO₄), and the solvent was removed under reduced pressure. The residue was chromatographed on silica using hexane as eluent. The solvent was removed under reduced pressure, and the residue was crystallized from hexane to give diphenylacetylene- I -¹³C- d_{10} (0.62 g, 33% from 2-phenylacetophenone- I -¹³C- d_{10}) as colorless needles. ¹³C NMR (75.45 MHz, CDCl₃): δ 89.73 (¹³C-acetylene). MS (EI): m/z 189 (M⁺, 100%).

Results and Discussion

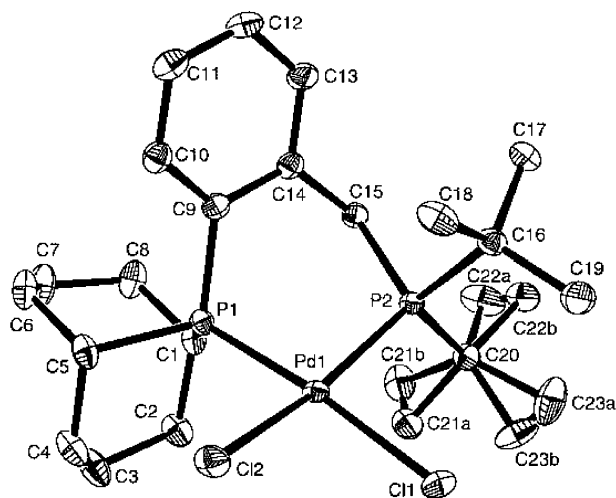
Preparation and Characterization of [Pd(bcope)(OTf)₂] (1a) and [Pd('bucope)(OTf)₂] (1b). The triflate complexes **1a** and **1b** [where bcope is (C₈H₁₄)PCH₂–CH₂P(C₈H₁₄) and 'bucope is (C₈H₁₄)PC₆H₄CH₂P('Bu)₂; both have been abbreviated as P₂ where necessary] were synthesized from their chloride analogues by the addition of AgOTf and isolated in good yield as pale yellow/white solids. The details of these syntheses and essential NMR data for these species can be found in the Experimental Section.

X-ray Diffraction Studies. The crystal and molecular structures of compounds [Pd('bucope)(Cl)₂] (see Figure 3 and Supporting Information), [Pd('bucope)(OH₂)₂](OTf)₂·2(H₂O)

(28) Eberhard, M. P. Ph.D. Thesis, University of Bristol, 2000.

(29) Marsh, P. Ph.D. Thesis, University of Bristol, 2003.

(30) Stang, P. J.; Cao, D. H.; Saito, S.; Arif, A. M. *J. Am. Chem. Soc.* **1995**, *117*, 6273–6283.



Cl(1)–Pd(1)	2.3632(5)	P(1)–Pd(1)–P(2)	90.497(19)
Cl(2)–Pd(1)	2.3594(5)	P(1)–Pd(1)–Cl(1)	173.440(14)
P(1)–Pd(1)	2.2485(5)	P(2)–Pd(1)–Cl(1)	91.99(2)
P(2)–Pd(1)	2.2953(5)	P(1)–Pd(1)–Cl(2)	90.42(2)
		P(2)–Pd(1)–Cl(2)	164.941(14)
		Cl(1)–Pd(1)–Cl(2)	88.75(2)

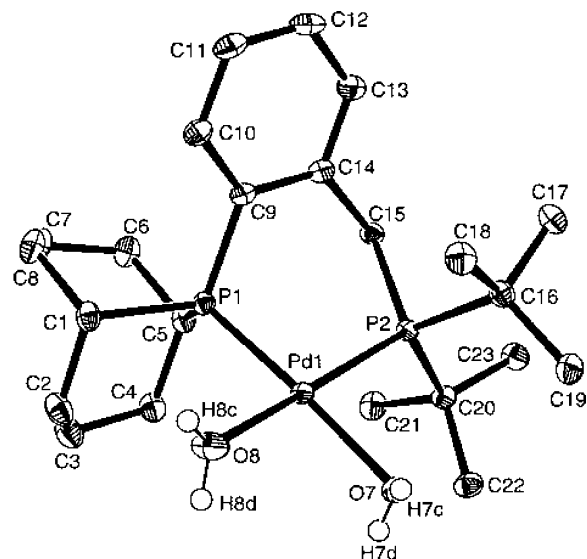
Figure 3. Molecular structure of $[\text{Pd}(\text{bucupe})\text{Cl}_2]$: ORTEP view showing 50% probability ellipsoids, and selected bond lengths (Å) and angles (°). Hydrogen atoms have been omitted for clarity.

(Figures 4 and 5) and $[\text{Pd}(\text{bcope})(\text{MeOH})_2](\text{OTf})_2 \cdot 2(\text{MeOH})$ (Figure 6) have been determined by X-ray diffraction studies. Selected crystallographic data for these complexes are presented in Table 1; complete crystallographic data for all three complexes are given in the Supporting Information. For all these structures, the hydrogens were placed using a riding model, except for the hydroxyl hydrogens, which were placed by difference map after all the other atoms had been positioned and refined.

Single-crystal X-ray-quality crystals of $[\text{Pd}(\text{bucupe})(\text{Cl})_2]$ were obtained by addition of diethyl ether to dichloromethane solutions of the solid. The palladium atom in this species is in the center of a square-planar arrangement of two chlorine and two *cis*-phosphorus atoms, and the P–Pd–P (90.497(19)°) angle is close to the ideal 90°. The Pd–Cl(1) and Pd–Cl(2) bond lengths are similar and comparable to Pd–Cl distances in other palladium bisphosphine dichloride complexes. While the position of the carbon atoms of one of the *tert*-butyl groups was disordered, two positions could be successfully modeled, the relative occupancy of which was refined to 45 and 55 respectively.

When **1b** was successfully crystallized by addition of diethyl ether to dichloromethane solutions, the cation actually proved to be the di-aqua complex, $[\text{Pd}(\text{bucupe})(\text{OH}_2)_2]^{2+}$. The palladium atom proved to be located in a distorted square-planar environment, with a phosphine bite angle P(1)–Pd(1)–P(2) of 90.049(16)°, which is very similar to that of the chloride precursor $[\text{Pd}(\text{bucupe})(\text{Cl})_2]$. The corresponding phosphorus–palladium distances are slightly shorter than those of the chloride, at 2.2343(4) and 2.2619(4) Å, rather than 2.2485(5) and 2.2953(5) Å, respectively, and confirm that the H_2O ligands have a poorer trans influence than chloride ligands.

Supramolecular Structure of $[\text{Pd}(\text{bucupe})(\text{OH}_2)_2](\text{OTf})_2 \cdot 2(\text{H}_2\text{O})$. Both water ligands in the cation $[\text{Pd}(\text{bucupe})(\text{OH}_2)_2]^{2+}$



O(1)–Pd(1)	2.1445(12)	P(1)–Pd(1)–P(2)	90.049(16)
O(2)–Pd(1)	2.1075(12)	O(1)–Pd(1)–P(1)	177.21(4)
P(1)–Pd(1)	2.2343(4)	O(1)–Pd(1)–P(2)	92.24(4)
P(2)–Pd(1)	2.2619(4)	O(2)–Pd(1)–P(1)	94.47(4)
		O(2)–Pd(1)–P(2)	168.50(4)
		O(2)–Pd(1)–O(1)	83.58(5)

Hydrogen bonds	d(D...A)	<(DHA)
O(1)–H(1B)...O(9)#1	2.6200(18)	173(3)
O(1)–H(1C)...O(3)#1	2.7469(19)	160(2)
O(2)–H(2C)...O(10)	2.5960(19)	171(3)
O(2)–H(2D)...O(5)#1	2.7443(19)	169(2)

Figure 4. Molecular structure of the cation $[\text{Pd}(\text{bucupe})(\text{OH}_2)_2]^{2+}$: ORTEP view showing 50% probability ellipsoids, and selected bond lengths (Å) and angles (°). Hydrogen atoms other than those of the H_2O ligands have been omitted for clarity.

are hydrogen-bonded to the same triflate and to two independent water molecules. In addition, these waters of crystallization are each bonded to a bridging triflate anion and to another independent triflate, as shown in Figure 5. The O–H...O distances are in agreement with those of related complexes,^{31–36} and similar hydrogen-bonding patterns have been described for other palladium aqua complexes with triflate counteranions.^{31,37,38} The hydrogen-bond networks constitute infinite chains parallel to the crystallographic *a*-axis.

When **1a** was successfully crystallized from cooled methanol solutions, the metal center contained two methanol solvates that were bound directly to palladium, in addition to a further pair which extended out to the two triflate counterions via appropriate hydrogen bonds. This species, $[\text{Pd}(\text{bcope})(\text{MeOH})_2](\text{OTf})_2 \cdot$

- (31) Qin, Z.; Jennings, M. C.; Puddephatt, R. J. *Inorg. Chem.* **2001**, *40*, 6220–6228.
- (32) Ruiz, J.; Florenciano, F.; Vicente, C.; De Arellano, M. C. R.; López, G. *Inorg. Chem. Commun.* **2000**, *3*, 73–75.
- (33) Ferrer, M.; Mounir, M.; Rossell, O.; Ruiz, E.; Maestro, M. A. *Inorg. Chem.* **2003**, *42*, 5890.
- (34) Gusev, O. V.; Kalsin, A. M.; Peterleitner, M. G.; Petrovskii, P. V.; Lyssenko, K. A.; Akhmedov, N. G.; Bianchini, C.; Meli, A.; Oberhauser, W. *Organometallics* **2002**, *21*, 3637–3649.
- (35) Vicente, J.; Arcas, A.; Bautista, O.; Jones, P. G. *Organometallics* **1997**, *16*, 2127–2138.
- (36) Stang, P. J.; Cao, D. H.; Poulter, G. T.; Arif, A. M. *Organometallics* **1995**, *14*, 1110–1114.
- (37) Stang, P. J.; Cao, D. H.; Saito, S.; Arif, A. M. *J. Am. Chem. Soc.* **1995**, *117*, 6273–6283.
- (38) Vicente, J.; Arcas, A. *Coord. Chem. Rev.* **2005**, *249*, 1135–1154.

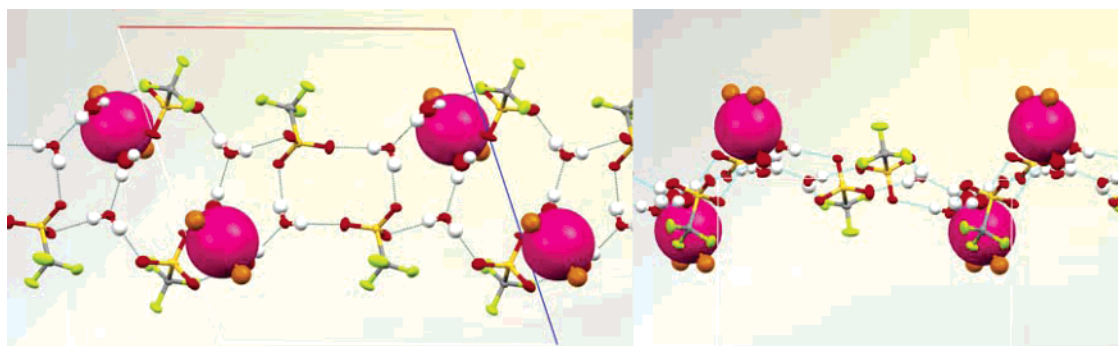
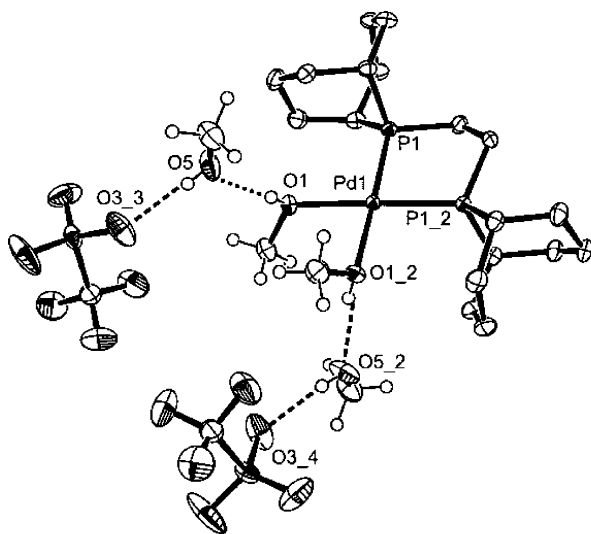


Figure 5. Views perpendicular to the *b* (left) and *c* (right) crystallographic axes of the supramolecular structure of $[\text{Pd}(\text{bucope})(\text{OH}_2)](\text{OTf})_2 \cdot 2(\text{H}_2\text{O})$, showing the hydrogen-bonding pattern. The cation units are represented by the metal center (big pink sphere), the phosphorus atoms, and the water ligands. Crystallization water molecules participate in the hydrogen-bonding pattern that build the infinite chains found along the crystallographic *a* axis.



O(1)–Pd(1)	2.1417(16)	O(1)#1–Pd(1)–O(1)	82.66(9)
P(1)–Pd(1)	2.2446(5)	P(1)#1–Pd(1)–P(1)	84.36(3)
		O(1)–Pd(1)–P(1)	96.54(5)
		O(2)–Pd(1)–P(2)	168.50(4)
Hydrogen bonds		d(D...A)	<(DHA)
O(5)–H(5A)...O(3)#2		2.670(3)	174(4)
O(1)–H(1A)...O(5)		2.615(3)	161(3)

Figure 6. Molecular structure of $[\text{Pd}(\text{bucope})(\text{MeOH})_2](\text{OTf})_2 \cdot 2\text{MeOH}$, including the hydrogen-bonding pattern: ORTEP view showing 50% probability ellipsoids, and selected bond lengths (Å) and angles (°). Hydrogen atoms other than those of the MeOH units have been omitted for clarity.

$2(\text{MeOH})$, therefore possesses a coordination environment of two *cis* phosphorus atoms and two oxygen atoms which belong to two independent methanol molecules. These crystals belong to the orthorhombic crystalline system, and the asymmetric unit contains a $\text{Pd}\{\text{PC}_8\text{H}_{14}\text{CH}_2\}(\text{MeOH})$ moiety, one triflate anion, and one methanol of crystallization. The rest of the atoms (denoted by “_2” or #) can therefore be generated by appropriate symmetry operations. In this species, the cation can be regarded as a solvento complex where two methanols have displaced the triflate counteranions from the palladium center.

The $\text{P}(1)–\text{Pd}–\text{P}(2)$ angle is significantly smaller in this species ($84.36(3)^\circ$) than in both $[\text{Pd}(\text{bucope})(\text{Cl})_2]$ and $[\text{Pd}(\text{bucope})(\text{OH}_2)_2](\text{OTf})_2 \cdot 2(\text{H}_2\text{O})$ ($90.497(19)$ and $90.049(16)^\circ$, respectively). In contrast, the $\text{P}–\text{Pd}$ distance of $2.2446(5)$ Å here is slightly longer than that in $[\text{Pd}(\text{bucope})(\text{OH}_2)_2](\text{OTf})_2 \cdot 2(\text{H}_2\text{O})$, $2.2343(4)$ Å.

The formation of palladium aqua complexes from the corresponding chlorides and silver or thallium salts is not rare, but there are relatively few reported structures of palladium triflate complexes, and there is only one reported example of the crystal structure of a bis-triflate complex.³⁹ However, it is well known that the triflate ligand can be easily replaced by water molecules present in or added to the solvent.^{36,38–40} Moreover, the formation of hydrogen-bonded networks clearly stabilizes such species with respect to the bis-triflate.^{41–43} To the best of our knowledge, only one structure for a palladium–methanol complex has been described previously.⁴⁴

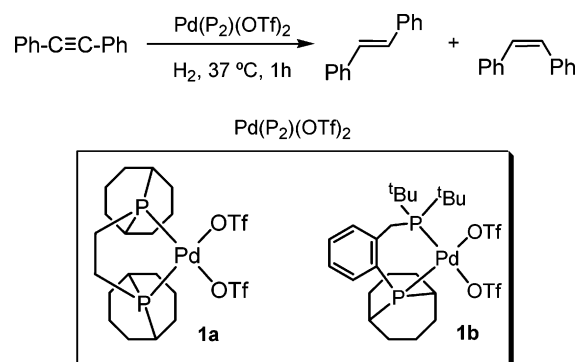
Hydrogenation of Diphenylacetylene in Methanol: Mechanistic Implications. Typical NMR experiments were completed in CD_2Cl_2 or methanol- d_4 containing the complex (**1a** or **1b**) and a 40-fold excess of diphenylacetylene- d_{10} . Three atmospheres of *para*-hydrogen was then introduced over the solution at 295 K, and the ensuing reaction was monitored by multi-nuclear NMR spectroscopy between 265 and 333 K. During these studies, the utilization of *p*- H_2 resulted in the observation of enhanced proton resonances for reaction products containing two hydrogen atoms that were originally present in a single *p*- H_2 molecule (Scheme 1). This effect provides information about the mechanism of reaction and is central to much of the work now reported.

In summary, the corresponding ^1H NMR spectra show weakly enhanced signals at the beginning of the experiments which correspond to the formation of *cis*-stilbene at δ 6.66, as well as unenhanced *trans*-stilbene at δ 7.18. These signals increase in intensity, relative to the background, during observation and hence correspond to reaction products that are essentially stable on the NMR time scale. Since the two alkene protons of the *cis* isomer are chemically and magnetically equivalent, the observation of a *p*- H_2 -enhanced emission signal at δ 6.66 is consistent with the involvement of an intermediate where two hydrogen atoms of the *p*- H_2 molecule become inequivalent.⁴⁵ The fact that the proton signal for *trans*-stilbene grows in intensity even

- (39) Anandhi, U.; Holbert, Y.; Lueng, D.; Sharp, P. R. *Inorg. Chem.* **2003**, 42, 1282.
- (40) Song, L. C.; Jin, G. X.; Zhan, W. X.; Hu, Q. M. *Organometallics* **2005**, 24, 700–706.
- (41) Rochon, F. D.; Melanson, R. *Inorg. Chem.* **1987**, 26, 989.
- (42) Braga, D.; Grepioni, F. *Acc. Chem. Res.* **1994**, 27, 51.
- (43) Braga, D.; Grepioni, F.; Sabatino, P.; Desiraju, G. R. *Organometallics* **1994**, 13, 3532.
- (44) Quek, G. H.; Leung, P.-H.; Mok, K. F. *Inorg. Chim. Acta* **1995**, 239, 185–188.
- (45) Aime, S.; Gobetto, R.; Canet, D. *J. Am. Chem. Soc.* **1998**, 120, 6770–6773.

Table 1. Selected Crystallographic Data for Pd(*tbucope*)Cl₂, [Pd(*bcope*)(MeOH)₂](OTf)₂·2MeOH, and [Pd(*tbucope*)(OH₂)₂](OTf)₂·2(H₂O)

	Pd(<i>tbucope</i>)Cl ₂	[1a (MeOH) ₂](MeOH)·2(OTf) ₂	[1b (OH ₂) ₂](OTf) ₂ ·2(H ₂ O)
formula	C ₂₃ H ₃₈ Cl ₂ P ₂ Pd	C ₂₄ H ₄₈ F ₆ O ₁₀ P ₂ PdS ₂	C ₂₅ H ₄₆ F ₆ O ₁₀ P ₂ PdS ₂
<i>M_r</i>	553.77	843.08	853.08
cryst size (mm)	0.24 × 0.16 × 0.08	0.15 × 0.13 × 0.11	0.24 × 0.23 × 0.20
cryst syst	monoclinic	orthorhombic	monoclinic
space group	<i>P</i> 2 ₁ / <i>c</i>	<i>P</i> 2 ₁ 2 ₁ 2	<i>P</i> 2 ₁ / <i>n</i>
cell constants			
<i>a</i> , Å	11.057(2)	10.1425(6)	14.8608(15)
<i>b</i> , Å	15.655(3)	12.0361(8)	16.6018(16)
<i>c</i> , Å	14.870(3)	14.1564(9)	14.8694(15)
α, deg	90	90	90
β, deg	109.911	90	108.403(2)
γ, deg	90	90	90
<i>V</i> , Å ³	2420.1(8)	1728.16(19)	3480.9(6)
<i>Z</i>	4	2	4
λ, Å	0.71073	0.71073	0.71073
ρ(calcd), Mg m ^{−3}	1.520	1.620	1.628
μ, mm ^{−1}	1.128	0.831	0.827
<i>F</i> (000)	1144	868	1752
<i>T</i> , K	115(2)	110(2)	100(2)
θ range, deg	1.95–28.30	2.22–30.03	1.69–30.04
no. of rflns measd	24424	19608	27146
no. of indep rflns	5994	4996	10013
max and min transmissn	1.000 and 0.873	0.913 and 0.845	1.000 and 0.624
<i>R</i> _{int}	0.0224	0.0247	0.0222
no. of restraints/params	0/290	0/214	0/453
<i>R</i> _w (<i>F</i> ²) (all rflns)	0.0514	0.0658	0.0646
<i>R</i> (<i>I</i>) (>2σ(<i>I</i>))	0.0229	0.0272	0.0260
<i>S</i>	1.054	1.056	1.029
largest diff peak and hole, e Å ^{−3}	0.578 and −0.545	0.679 and −0.466	0.607 and −0.419

Scheme 1

though this signal does not show *p*-H₂ enhancement is consistent with it being the thermodynamically preferred product.

When such reactions are examined using ¹³C-enriched diphenylacetylene-*d*₁₀, the δ 6.66 signal is strongly enhanced, while the δ 7.18 signal shows limited PHIP enhancement. These effects arise because both of the two alkenic protons of *cis*- and *trans*-PhCH=¹³CHPh are magnetically inequivalent due to the presence of the ¹³C label, and efficiently enhanced NMR transitions are now observed.

The % conversion obtained after 1 h was determined by GC/MS when 2 mg of catalyst was added to a 50-fold excess of substrate in 1 mL of solvent and the resultant reaction with 3 atm of H₂ was initiated at 312 K. These data (see Supporting Information) confirm that (i) the hydrogenation activity is greater in methanol than CD₂Cl₂, (ii) **1b** favors the formation of *trans*-stilbene, and (iii) **1b** is more active than **1a**. It also reveals that **1a** shows a higher degree of C–C coupling products. It should also be noted that, when these reactions were completed in methanol-*d*₄, essentially no deuteration of the products was observed according to the GC/MS fragmentation patterns. In a related study, Cole-Hamilton et al. demonstrated the participa-

tion of a cationic hydride complex in the formation of methyl propanoate from CO and ethane. This work was completed in deuterated methanol, and evidence was presented that Pd–H/CH₃OD exchange was slow relative to propagation.⁴⁶ We will return to this point later in the manuscript.

The mechanistic routes taken to form these species are now discussed explicitly.

Inorganic Complex Speciation 1. Reactions of Pd(*bcope*)-(OTf)₂ (1a**) with *p*-H₂ and Diphenylacetylene in CD₂Cl₂.** We have previously described the finding that, when a 1 μM solution of **1a** in CD₂Cl₂ containing a 50-fold excess of diphenylacetylene-*d*₁₀ is placed under 3 atm of 100% *p*-H₂ at 213 K and rapidly introduced into a 400 MHz NMR spectrometer, a new palladium complex is detected.²⁴ The studies now described demonstrate that this corresponds to the cation [Pd(*bcope*)-(CHPhCH₂Ph)](OTf) (**2a**) and not Pd(*bcope*)(CHPhCH₂Ph)(H) as originally suggested.

The starting ³¹P{¹H} NMR spectrum contains a singlet at δ 73.11 due to **1a**, but the most notable feature of the corresponding ¹H NMR spectrum of **2a** is the observation of substantially enhanced proton signals at δ 4.94 and δ 3.13, and a further weakly enhanced signal at δ 2.92 (Table 2). These signals contained characteristic antiphase components due to their origin as protons in *p*-H₂, proved to be coupled in a COSY spectrum, and simplified on ³¹P decoupling. ¹H–³¹P heteronuclear multi-quantum coherence (HMQC) spectra then revealed that this species yielded two ³¹P doublets at δ 32.3 and δ 42.9 (*J*_{PP} = 47 Hz). A ¹H–¹³C HMQC spectrum produced correlations from the proton resonance at δ 4.94 to a ¹³C signal at δ 63.0, with the remaining proton resonances connecting to a signal at δ 37.1. We therefore concluded that these resonances arise from a ligand that is attached to palladium. When this reaction was

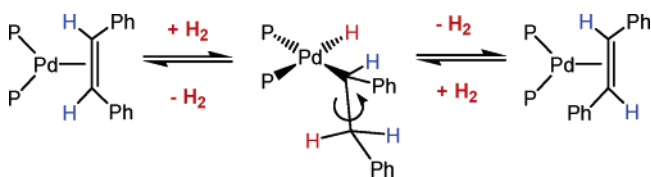
(46) Eastham, G. R.; Tooze, R. P.; Kilner, M.; Foster, D. F.; Cole-Hamilton, D. J. *Dalton Trans.* **2002**, 1613–1617.

Table 2. Selected ^1H , ^{31}P , and ^{13}C NMR Data for Complexes **2–7** at 298 K as a Function of Solvent

	δ ^1H		δ ^{31}P		δ ^{13}C	
	in CD_2Cl_2	in methanol- d_4	in CD_2Cl_2	in methanol- d_4	in CD_2Cl_2	in methanol- d_4
Pd(bcope)$^{2+}$ System						
2a	4.94 (CHPh); 3.13, 2.92 (CH_2Ph)	4.98 (CHPh); 3.06, 2.89 (CH_2Ph)	32.30, 42.90 (d, $J_{\text{PP}} = 47$ Hz)	32.20, 43.40 (d, $J_{\text{PP}} = 40$ Hz)	63.0 (CH), 37.1 ($J_{\text{CP}} = 42$, 14 Hz; CH_2)	62.30 (dd, $J_{\text{CP}} =$ 54, 16 Hz; CH), 35.60 (dd, $J_{\text{CP}} =$ 16, 5 Hz; CH_2) 161.2 (CPh=), 130.6 ($=\text{CH}_2\text{Ph}$)
3a		6.75 (dd, $J_{\text{HP}} =$ 13.6, 6.8 Hz)		21.79 (m, trans to vinyl), 39.04 (cis to vinyl)		129.9 (d, $J_{\text{CP}} =$ 18 Hz; CPh=), 163.3 (dd, $J_{\text{CP}} =$ 109, 10 Hz; $=\text{CH}_2\text{Ph}$)
4a	6.72 (dd, $J_{\text{HP}} =$ 13.2, 5.6 Hz)	6.70 (dd, $J_{\text{HP}} =$ 12.7, 5.2 Hz)	19.70 (trans to hydride), 33.51 (cis to hydride)	20.17 (m, trans to vinyl), 33.41 (cis to vinyl)		
5a	−7.04 (dd, $J_{\text{HP}} =$ 223.2, 19.0 Hz)	−6.96 (dd, $J_{\text{HP}} =$ 232.3, 17.2 Hz)	22.33 (d, $J_{\text{PP}} =$ 22 Hz, cis to hydride), 43.40 (trans to hydride)			
6	−6.40 (ddd, $J_{\text{HP}} =$ 190.7, 25.3, 11.6 Hz)	−6.30 (ddd, $J_{\text{HP}} =$ 191.1, 23.8, 12.9 Hz)	28.1, 57.4			
Pd('bcope)$^{2+}$ System						
2b	4.92 (CHPh); 3.02, 2.95 (CH_2Ph)	4.93 (CHPh); 3.03, 2.91 (CH_2Ph)	70.70 (P^tBu_2 trans to alkyl), 20.40	70.43 (P^tBu_2 trans to alkyl), 19.81 ($J_{\text{PP}} = 60$ Hz)	63.94 (CHPh) 35.98 (CH_2Ph)	64.0 (d, $J_{\text{CP}} =$ 55 Hz; CH), 34.8 (CH_2)
3b		6.72 (dd, $J_{\text{HP}} =$ 12.0, 8.9 Hz)				
4b	6.61 (dd, $J_{\text{HP}} =$ 11.4, 8.4 Hz)	6.62 (dd, $J_{\text{HP}} =$ 11.7, 8.8 Hz)		15.11 (d, $J_{\text{PP}} =$ 42 Hz), 57.62 (d, $J_{\text{PP}} = 42$ Hz)		128.6 (CPh=), 163.9 (d, $J_{\text{CP}} =$ 101 Hz; $=\text{CH}_2\text{Ph}$)
5b	−7.77 (dd, $J_{\text{HP}} =$ 208.5, 9.7 Hz)	−7.69 (major) (dd, $J_{\text{HP}} = 209.4$, 8.3 Hz)	−2.20 (d, $J_{\text{HP}} =$ 24 Hz, trans to hydride), 100.96	−2.54 (d, $J_{\text{HP}} =$ 27 Hz, trans to hydride), 101.92 (d, $J_{\text{HP}} = 27$ Hz, trans to pyridine)		
5b'	−7.91 (dd, $J_{\text{HP}} =$ 205.2, 13.5 Hz)	−7.84 (minor) (dd, $J_{\text{HP}} = 205.5$, 13.3 Hz)				
7	−4.21 (ddd, $J_{\text{HH}} =$ 18.0 Hz; $J_{\text{HP}} = 138$, 9 Hz; trans to P^tBu_2), −4.71 (ddd, $J_{\text{HH}} =$ 18.0 Hz; $J_{\text{HP}} = 146$, 9 Hz; trans to PC_8H_{11})					

re-examined using $^{13}\text{C}\equiv\text{C}$ -enriched diphenylacetylene- d_{10} , strong signals were observed in the one-dimensional, fully coupled ^{13}C NMR experiment at δ 63.0 and δ 37.1; the former showed two ^{31}P splittings of 42 and 14 Hz in addition to a single proton splitting of 147 Hz. The δ 63.0 signal therefore corresponds to a CH group that is bound directly to palladium. In this spectrum, the δ 37.1 signal appears as a pseudo-triplet as a consequence of the PHIP effect, with lines of relative intensities 1, 0, and −1, and therefore it corresponds to a CH_2 moiety ($J_{\text{CH}} = 130$ Hz). This would be consistent with the fact that *cis*-Ph-CH=CH-Ph has been converted into a CHPhCH $_2$ Ph group which is bound to the metal.

In order to explore the reactivity of **2a**, a series of modified one-dimensional exchange spectroscopy (1D EXSY) experiments were recorded where a single alkyl proton resonance was selected and magnetization transfer from this site monitored as a function of mixing time. For the δ 4.94 peak, strong magnetization transfer into the *trans*-stilbene signal at δ 7.18 was observed at 295 K. When the sample was warmed to 313 K, even greater magnetization transfer from the δ 4.94 site into *trans*-stilbene was seen in conjunction with weaker transfer into *cis*-stilbene and into both of the previously described CH_2Ph proton sites at δ 3.13 and δ 2.92. When the peak at δ 3.13 was

Scheme 2. Proposed Mechanism for Alkene Isomerization Based on Neutral Intermediates

selected in an analogous EXSY experiment at 313 K, exchange into free H_2 , and weaker exchange into free *cis*- and *trans*-stilbene as well as into the δ 4.94 position of **2a**, was observed. However, when the resonance at δ 2.92 was selected, only transfer into *trans*-stilbene was seen. These observations confirm that the proton yielding the resonance at δ 3.13 transfers directly into free H_2 , while those at δ 4.94 and δ 2.92 move into *trans*-stilbene. In our earlier report,²⁴ these data were taken to indicate that **2a** was an alkyl hydride, even though the hydride resonance itself was not observed (Scheme 2). This deduction was supported by a number of theoretical calculations.²⁵

Inorganic Complex Speciation 2. Reactions of Pd(bcope)-(OTf) $_2$ (1a**) with *p*- H_2 and Diphenylacetylene in Methanol- d_4 . (a) Identification of **2a** as the Cation Pd(bcope)-(CHPhCH $_2$ Ph) $^+$.** A sample containing **1a**, diphenylacetylene-

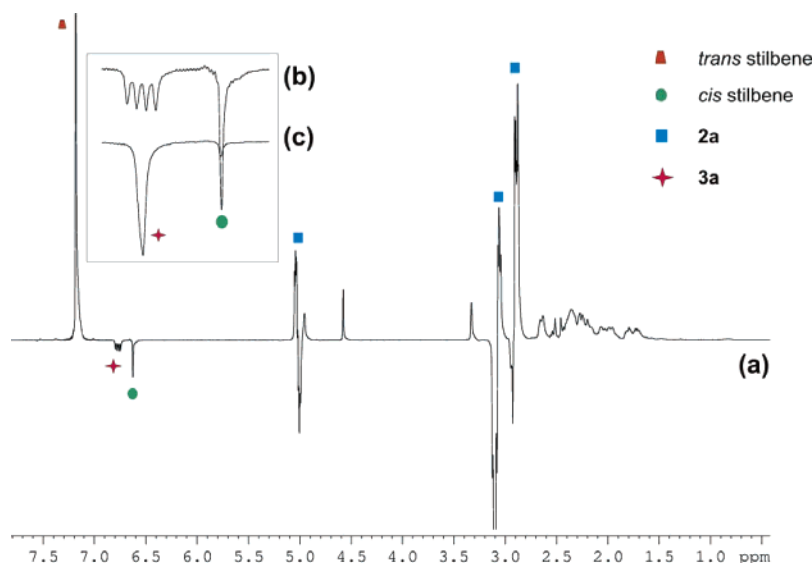


Figure 7. (a) ^1H NMR spectra for the reaction of **1a** with diphenylacetylene- d_{10} and $p\text{-H}_2$ in methanol- d_4 , showing ^1H resonances for *trans*-stilbene, *cis*-stilbene (in emission), antiphase PHIP signals for the alkyl protons of **2a**, and an emission doublet of doublets for the vinyl proton of **3a**. In the expanded inset traces, the effect of broadband ^{31}P decoupling (c) on the emission resonances for *cis*-stilbene and the vinyl proton of **3a** is illustrated (b).

d_{10} , and $p\text{-H}_2$ in methanol- d_4 was prepared and monitored by NMR spectroscopy. The starting $^{31}\text{P}\{^1\text{H}\}$ NMR spectrum contained a singlet at δ 72.12 due to the methanol solvate of **1a**. The corresponding ^1H NMR spectrum yielded signals for the same organic products as observed in CD_2Cl_2 and enhanced proton signals due to the palladium-based species **2a** at δ 4.98, 3.06, and 2.89 that were now of much greater intensity, in accordance with a much higher hydrogenation activity, but there were still no signals seen in the hydride region of the ^1H NMR spectrum (Figure 7). These three proton NMR signals still contained the characteristic antiphase components seen in CD_2Cl_2 and were all mutually coupled. Now, the PHIP-enhanced δ 4.98 signal clearly possesses two J_{HH} couplings of 11.5 and 4.0 Hz and two ^{31}P splittings of 10.6 and 4.3 Hz, which can be removed by appropriate ^{31}P decoupling. The corresponding ^1H – ^{31}P HMQC spectrum, which utilizes magnetization transfer from the three enhanced proton resonances, showed two ^{31}P doublets at δ 43.40 and δ 32.20 (d, $J_{\text{PP}} = 40$ Hz). Two ^{13}C signals were also located for this species in methanol- d_4 , at δ 62.30 (dd, $J_{\text{CP}} = 54.0$ and 16.0 Hz, CH) and δ 35.60 (dd, $J_{\text{CP}} = 16.0$ and 5.0 Hz, CH_2). The chemical shifts of the enhanced proton resonances, and the associated ^{31}P and ^{13}C signals of **2a** seen in methanol- d_4 , are therefore very similar to those seen in CD_2Cl_2 (Table 2). This suggests that **2a** does not contain bound solvent.

Species **2a** is therefore minimally described as $\text{Pd}(\text{bcope})\text{-(CHPhCH}_2\text{Ph)}$. This moiety would, however, be paramagnetic, and **2a** must therefore either be cationic or, as suggested in our previous report,²⁴ contain a hydride ligand, which is not observed. We thought that this situation was not too surprising since the successful observations of palladium hydride resonances are relatively rare and their appearance is very temperature-sensitive. Furthermore, we note that, for the PHIP effect to operate in the traditional way for two inequivalent protons, we need a resolvable H^*-H^* coupling, which in this case would be vanishingly small for the necessary four-bond $\text{Pd}(\text{H}^*)\text{-(CHPhCHH}^*\text{Ph)}$ connection. We also recorded a ^{31}P insensitive nuclei enhanced by polarization transfer (INEPT) spectrum, where a hydride coupling should be retained. The ^{31}P resonance

of **2a** at δ 32.20 showed substantial broadening, which we originally took to indicate the presence of such a ligand. The earlier demonstration of the concomitant elimination of H_2 and *trans*-stilbene from **2a**, and the fact that the hydrogenation products contain only additional ^1H labels, even in methanol- d_4 , were taken as additional indirect proof, but surprisingly, an alternative, more complex explanation for these observations was revealed when we continued to explore the reactivity of the methanol system.

In the related cationic bis-phosphine complex $\text{Pd}(\text{1,2-(CH}_2\text{P}^+\text{Bu}_2)_2\text{C}_6\text{H}_4)(\text{CH}_2\text{CH}_3)^+$, the ethyl ligand interacts with the metal center by an agostic C–H interaction from the β carbon.² An alternative situation has been reported in related cationic benzylpalladium systems featuring coordination of the pendant arene to the metal center.^{8,47}

Since the chemical shifts of the alkyl ligand resonances in **2a** are remarkably similar in CD_2Cl_2 and methanol- d_4 , coordination of the solvent or water is unlikely.⁴⁸ Values of J_{HC} have been used extensively to assess such agostic interactions,^{49–51} and the corresponding proton–carbon coupling constants for the CH and CH_2 carbons of the alkyl ligand in **2a** are 151 and 130 Hz, respectively. While these values are similar to those reported by Heaton et al. for the palladium ethyl system,¹⁰ they are relatively large for an agostic interaction.

In order to establish the exact nature of **2a**, full characterization of the proton and carbon resonances for the alkyl ligand is necessary. An NMR sample of **1a** (3 mg) and protio-*cis*-stilbene (12 μL) in methanol- d_4 was therefore prepared, cooled to 258 K, and reacted with H_2 (3 atm). The slow conversion of **1a** into **2a** was followed by ^1H and ^{31}P NMR spectroscopy. The

(47) Hii, K. K. M.; Claridge, T. D. W.; Giernoth, R.; Brown, J. M. *Adv. Synth. Catal.* **2004**, *346*, 983–988.

(48) CD_2Cl_2 was carefully dried from calcium hydride and stored with 4 Å molecular sieves in the absence of light. Methanol- d_4 was similarly dried with iodine and magnesium turnings. When samples of **1a** and diphenylacetylene were prepared using these solvents, no changes in the chemical shift of the detected intermediates were observed.

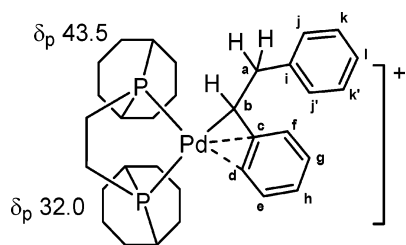
(49) Brookhart, M.; Green, M. L. H. *J. Organomet. Chem.* **1983**, *250*, 395–408.

(50) Crabtree, R. H. *Angew. Chem., Int. Ed. Engl.* **1993**, *32*, 789–805.

(51) Shultz, L. H.; Tempel, D. J.; Brookhart, M. *J. Am. Chem. Soc.* **2001**, *123*, 11539–11555.

Table 3. Selected NMR Data Obtained for **2a** in Methanol-*d*₄ at 258 K

assignment	δ ¹ H	assignment	δ ¹³ C
a	3.13, 2.94	a	35.5 ($J_{CP} = 5$ Hz)
b	5.11 ($J_{HH} = 5$ Hz, $J_{HP} = 5$ Hz, $J_{HC} = 144$ Hz)	b	62.7 ($J_{CP} = 12, 44$ Hz)
d	6.98 ($J_{HH} = 5$ Hz, $J_{HP} = 5$ Hz, $J_{HC} = 143$ Hz)	c	119.0 (t, $J_{CP} = 6$ Hz)
e	8.02 ($J_{HC} = 162$ Hz)	d	105.4 (d, $J_{CP} = 14$ Hz)
f	7.54	e	134.2
g	7.05	f, h	129.2/132.2 ($J_{CP} = 3$ Hz)
h	7.54	g	129.1
j, j'	7.12	i	141.0 (t, $J_{CP} = 10$ Hz)
k, k'	7.21	j, j'	128.4
l	7.18	k, k'	127.8
		l	126.0

Chart 1. Proposed Structure for **2a**

additional NMR data obtained for **2a** are presented in Table 3. The most significant feature of the ¹H NMR spectrum corresponded to the observation of five distinct resonances for one of the phenyl rings of the alkyl ligand, which indicates that there is restricted rotation about the corresponding C–C bond. Four of these protons coupled to the δ 43.5 ³¹P signal arising from the phosphorus center, which is cis to the alkyl ligand in the corresponding ¹H–³¹P spectrum. The size of the corresponding ortho-phenyl proton–phosphorus splitting was 5 Hz. In the corresponding ¹H–¹³C spectrum, the ortho proton connected with a ¹³C center at δ 105.4 which possesses a ³¹P splitting of 14 Hz; in addition, it showed NOE connections to the δ 5.11 proton of the alkyl, thereby confirming that the phenyl group was on the α -carbon of the alkyl. The correspond J_{HC} value was determined to be 143 Hz. The ipso carbon of the phenyl ring showed a triplet ³¹P splitting of 6 Hz, in accord with this deduction. These data provide unambiguous evidence that the palladium center interacts with the π -system of the arene rather than the C–H bond. We therefore conclude that **2a** is stabilized by metal–ring association, as illustrated in Chart 1.⁴⁷

(b) Detection of the Vinyl Complex [Pd(bcpo)(CPh=CHPh)(MeOH)](OTf) (3a**).** In the early stages of this reaction, when the catalytic activity of the system is optimal, a weak emission signal appears as a doublet of doublets at δ 6.75 (13.5 and 6.8 Hz) in methanol-*d*₄; this signal is not seen in CD₂Cl₂. This new signal becomes a singlet on ³¹P decoupling, and consequently the two splittings must arise from interactions with

two inequivalent ³¹P centers (Figure 7). When such a sample is cooled to 275 K, this emission signal grows in strength and can ultimately be seen as a normal NMR signal from a thermally equilibrated spin system. In contrast, the associated resonances for **2a** were only visible in the associated ¹H NMR spectra because of the PHIP effect. This observation agrees with the fact that, when a ³¹P{¹H} NMR spectrum was recorded, in addition to the dominant signal for **1a**, two doublets appeared at δ 39.04 and δ 21.75, with $J_{PP} = 40.0$ Hz. In the corresponding ¹H–³¹P HMQC experiment, these signals coupled to the ¹H signal at δ 6.75, with the former resonance providing the 13.6 Hz splitting.

Before we identify this species (**3a**), we must first comment on the fact that the δ 6.75 signal appears in emission. Such a situation also occurs for the cis isomer of stilbene, where the two alkene protons are chemically and magnetically equivalent and appear at δ 6.66. In this case, the involvement of an intermediate in the formation of *cis*-stilbene is indicated, where two hydrogen atoms of the original *p*-H₂ molecule become inequivalent but are then transported into the final, symmetrical environment;⁴⁵ in other words, “*para-cis*-stilbene” is formed. The binding of *cis*-CHPh=CHPh to palladium would meet this requirement, but the corresponding proton resonances of Pd-(bcpo)(η^2 -CHPh=CHPh) would be expected to appear around δ 5, and only single ³¹P and alkenenic ¹³C signals should be observed for this species.^{7,52,53}

We therefore proceeded to record a ¹H–¹³C HMQC spectrum using ¹³C-enriched diphenylacetylene-*d*₁₀ to confirm the exact nature of **3a**. These spectra were recorded at 313 K and showed two ¹³C resonances, at δ 130.6 and δ 161.2, coupled to the proton resonance of **3a** at δ 6.75. The carbon resonance at δ 161.2 is indicative of a vinyl carbon signal, but the poor resolution prevented the detection of diagnostic carbon–phosphorus couplings that would confirm this. Nonetheless, this suggests that **3a** has the form [Pd(bcpo)(*cis*-CPh=CHPh)], and the remaining coordination site must correspond to either a hydride ligand if the complex is neutral or methanol if it is cationic. Furthermore, the emission signal arises from a single proton that was previously found in *para*-hydrogen. This effect has been seen before and has been referred to as a one-proton PHIP.⁵⁴ On the basis of the fact that we have previously identified *cis*-Pd(PEt₃)₂(CPh=CHPh)(H) through enhanced and coupled hydride and vinyl signals, and that these are not seen this time, we believe that **3a** is the cation [Pd(bcpo)(*cis*-CPh=CHPh)(MeOH)](OTf). This species can be observed in CD₂-Cl₂ if 10 μ L of methanol-*d*₄ is added to the reacting solution. A similar complex can be detected when ethanol rather than methanol is added to the solution (δ 6.76 at 313 K, $J_{HP} = 14.6$, 9.2 Hz).

A series of 1D EXSY experiments were then used to probe magnetization transfer within **2a** in methanol-*d*₄. Selective irradiation of the ¹H signals at δ 4.98 and δ 2.98 led to transfer into *trans*-stilbene. Interestingly, excitation of the remaining resonance at δ 3.06 revealed exchange into the δ 6.75 signal due to **3a** and not into free H₂, as seen in CD₂Cl₂.

(52) Liu, W.; Brookhart, M. *Organometallics* **2004**, *23*, 6099–6107.(53) Bruner, T. J.; Blank, N. F.; Moncarz, J. R.; Scriban, C.; Anderson, B. J.; Glueck, D. S.; Zakharov, L. N.; Golen, J. A.; Sommer, R. D.; Incavito, C. D.; Rheingold, A. L. *Organometallics* **2005**, *24*, 2730–2746.(54) Permin, A. B.; Eisenberg, R. *J. Am. Chem. Soc.* **2002**, *124*, 12406–1407.

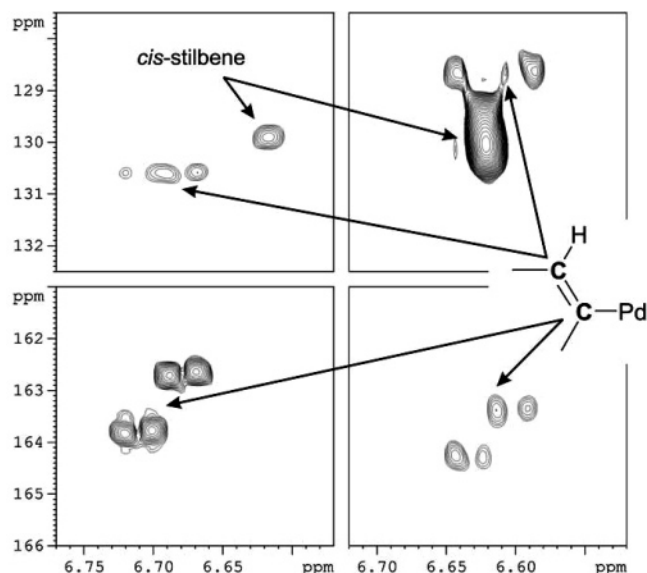


Figure 8. ^1H – ^{13}C HMQC NMR spectra, optimized for long-range correlations, illustrating the connection between the vinylic protons of **4a** (left) and **4b** (right) and the two vinyl carbon signals.

In order to test for the presence of bound solvent, in this case methanol in **3a**, we decided to add pyridine to the reaction mixture. We now describe those results.

(c) Reactions of Pd(bcope)(OTf)₂ (1a) with *p*-H₂ and Diphenylacetylene in Methanol-*d*₄ Containing 2 μL of Pyridine. A methanol-*d*₄ sample of **1a** containing *p*-H₂, diphenylacetylene, and 2 μL of pyridine was prepared. At the start of the experiment, the $^{31}\text{P}\{^1\text{H}\}$ NMR spectrum contained a singlet at δ 57.65, which suggests that the Pd(bcope)(OTf)₂ is converted into the pyridine solvate [Pd(bcope)(pyridine)₂](OTf)₂. When the corresponding reaction was monitored 295 K, much weaker polarization was observed, although when the sample was warmed to 305 K, **2a** could be readily characterized. Since the corresponding ^1H and ^{31}P resonances for **2a** are almost identical to those seen in methanol-*d*₄ or CD₂Cl₂, we believe that **2a** does not contain pyridine, methanol, or CD₂Cl₂ within its coordination sphere as discussed before. However, we now see two enhanced emission signals, one at δ 6.70 (dd, J_{HP} = 12.7, 5.2 Hz) due to **4a** and a second at δ –6.96 (dd, J_{HP} = 232.3, 17.2 Hz) due to a new species, **5a**. Both of these proton signals collapse into singlets upon broadband ^{31}P decoupling. Furthermore, as the reaction progresses, a second hydride resonance, also emissive, appears at δ –6.30 due to **6**, which has a doublet of doublets of doublets multiplicity due to coupling to three ^{31}P nuclei, where the corresponding splittings are 191.1, 23.8, and 12.9 Hz.

The δ 6.70 signal of **4a** couples to two ^{31}P centers which appear at δ 20.17 and δ 33.41 in the corresponding ^1H – ^{31}P HMQC experiment. These differ from those seen for **3a** in methanol-*d*₄, which appear at δ 21.79 and δ 39.04, and suggest that **4a** is the cation [Pd(bcope)(*cis*-CPh=CHPh)(pyridine)](OTf). This was confirmed when ^{15}N -labeled pyridine was employed, since in that case the ^{31}P resonance at δ 33.41 showed an extra 17 Hz splitting. This also provides further support that **3a** is indeed [Pd(bcope)(*cis*-CPh=CHPh)(MeOD)](OTf).

Unfortunately, because of low signal strengths and short lifetimes, it was not possible to determine the chemical shift of the phosphorus resonances for the bound bcope ligand in **5a**

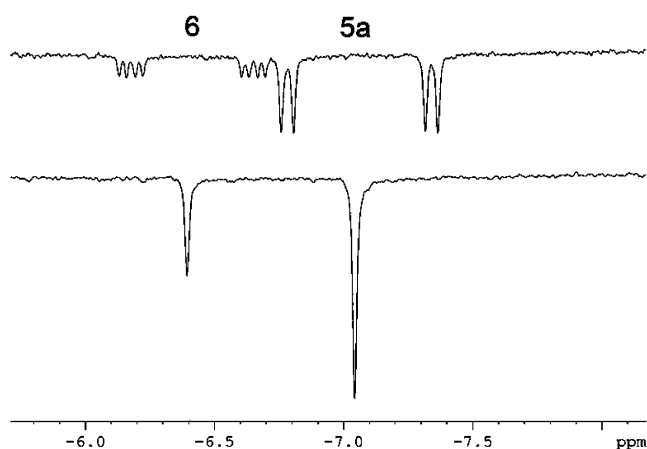


Figure 9. Hydride region of ^1H (upper trace) and $^1\text{H}\{^{31}\text{P}\}$ (lower trace) NMR spectra obtained during the reaction of **1a** with diphenylacetylene-*d*₁₀, pyridine, and *p*-H₂ in CD₂Cl₂ at 313 K. The emission signals for the hydride resonances of **5a** (right) and **6** (left) are illustrated.

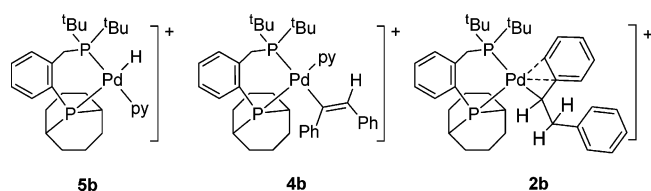
and **6** in methanol. However, when ^{15}N -labeled pyridine was employed, the signal at δ –6.96 showed some evidence of broadening, although a discrete ^{15}N splitting was not observed. Nonetheless, species **5a** is proposed to be the cation [Pd(H)-(bcope)(pyridine)](OTf).

The corresponding ^1H – ^{13}C HMQC spectrum of **4a** in methanol-*d*₄, obtained using the ^{13}C -enriched diphenylacetylene-*d*₁₀, showed two resonances at δ 129.9 (d, J_{CP} = 18 Hz) and δ 163.3 (dd, J_{CP} = 109, 10 Hz). The improved resolution confirms that the δ 163.3 signal corresponds to a vinyl carbon with phosphorus couplings that indicate it is bound to palladium (Figure 8).

Modified 1D EXSY experiments were then used to probe magnetization transfer within **2a**, and selective irradiation of the ^1H signals at δ 4.98 and δ 2.89 led to transfer into *trans*-stilbene. Interestingly, excitation of the remaining resonance at δ 3.06 revealed exchange into the δ 6.70 signal due to **3a** and the δ –6.96 signal due to **5a**. These data are consistent with a cationic reaction cycle based on **2a** being Pd(bcope)(CHPhCH₂-Ph)(OTf) rather than a neutral cycle based on Pd(bcope)-(CHPhCH₂Ph)(H).

(d) Reactions of Pd(bcope)(OTf)₂ (1a) with *p*-H₂ and Diphenylacetylene in CD₂Cl₂ Containing 2 μL of Pyridine. When the reaction of **1a** with *p*-H₂ and diphenylacetylene is monitored in CD₂Cl₂ with 2 μL of pyridine, no polarization was visible until the temperature reached 313 K. The initial $^{31}\text{P}\{^1\text{H}\}$ NMR spectrum contained a singlet at δ 54.30, which suggests that the Pd(bcope)(OTf)₂ is converted into the pyridine solvate [Pd(bcope)(pyridine)₂](OTf)₂ prior to the start of the reaction. This species then reacts relatively slowly at 313 K, and ultimately the PHIP-enhanced signals of **2a** become visible. In addition, ^1H NMR signals for *cis*- and *trans*-stilbene are again observed, but now a doublet of doublets appears at δ 6.72 (J_{HP} = 13.2, 5.6 Hz) due to **4a** and a hydride signal appears at δ –7.04 (dd, J_{HP} = 223.2, 19.0 Hz) due to **5a**. Both of these resonances appear as enhanced emission signals, and as the reaction proceeds a second hydride resonance appears at δ –6.40 due to **6**. These spectral features are illustrated in Figure 9. The addition of pyridine to the CD₂Cl₂ solvent system therefore facilitates the detection of the cationic vinyl and hydride products. The lower activity of the CD₂Cl₂-based system

Chart 2



tuted phosphorus center. ^{13}C – ^1H HMQC experiments, using ^{13}C -enriched diphenylacetylene- d_{10} as the substrate, enabled the ^1H resonance of **2b**, which appears at δ 4.93, to be connected to a ^{13}C signal at δ 64.0 (d, $J_{\text{CP}} = 55$ Hz), while the proton at δ 2.91 for the CH_2 group connected to a signal at δ 34.8. The structure of **2b** shown in Chart 2 reflects an arene π coordination motif similar to that deduced for **2a**.

When the reaction of $\text{Pd}(\text{t}^{\text{Bu}}\text{cope})(\text{OTf})_2$ (**1b**) with diphenylacetylene- d_{10} and $p\text{-H}_2$ was followed in methanol- d_4 at 298 K, in addition to the signals of **2b** already described, an emission signal was seen at δ 6.72 in the proton spectrum which possessed two phosphorus splittings of 8.9 and 12.0 Hz. The formation of $[\text{Pd}(\text{t}^{\text{Bu}}\text{cope})(\text{CPh}=\text{CHPh})(\text{MeOH})](\text{OTf})$ (**3b**) is therefore indicated. NMR data for **3b** are presented in Table 2 (below). The analogous emission signal was not seen in CD_2Cl_2 .

Inorganic Complex Speciation 4. $\text{Pd}(\text{t}^{\text{Bu}}\text{cope})(\text{OTf})_2$ (1b**): Effect of Pyridine.** A series of analogous reactions in methanol- d_4 and CD_2Cl_2 with **1b**, diphenylacetylene, and *para*-hydrogen in the presence of 2 equiv of pyridine were carried out. In these experiments, polarized resonances were always seen for the alkyl ligand of **2b**. Two emission signals were also detected in these reactions, one at δ 6.62 (or δ 6.61 in CD_2Cl_2) for **4b** ($T = 303$ K using CD_2Cl_2 and 295 K with methanol- d_4) and one at δ –7.77 for **5b** (in CD_2Cl_2 , Figure 11). As expected, the hydride signal possessed a large trans phosphorus coupling of 208.5 Hz and a small cis phosphorus coupling of 9.7 Hz. When the signal-to-noise ratio observed for this resonance became substantial, a much weaker second hydride was seen at δ –7.91 (**5b'**) with similar multiplicity and J_{PH} values of 205.2 and 13.5 Hz.

The spectroscopic data for these species in both solvents are listed in Table 2. The characterization of the vinyl- and hydride-based species is also complicated by the symmetry of the phosphine, and, not surprisingly, when a ^1H – ^{31}P HMQC experiment was recorded in CD_2Cl_2 , two mutually coupled doublets were located for **5b** at δ –2.2 ($J_{\text{PP}} = 24$ Hz) and δ 100.96. The former signal arises from the cyclooctane-substituted phosphorus center, while the latter is due to the ^tBu -substituted group. Unfortunately, the weakness of the hydride signal for **5b'** prevented the analysis of the corresponding ^{31}P information, but when a ^1H NMR spectrum was collected with selective phosphorus decoupling around δ –2.2, the large hydride–phosphorus coupling was removed for the hydride resonance of **5b** and the small one for **5b'**. When this experiment was repeated with irradiation around δ 100 in the ^{31}P spectrum, the reverse happened: the small coupling was removed for the hydride resonance of **5b** and the large coupling for **5b'**. We therefore conclude that **5b** and **5b'** are simply isomers that differ according to the relative orientations of the hydride, pyridine, and phosphorus ligands.

A remarkable feature of these experiments is the observation in CD_2Cl_2 of a set of weakly enhanced hydride resonances

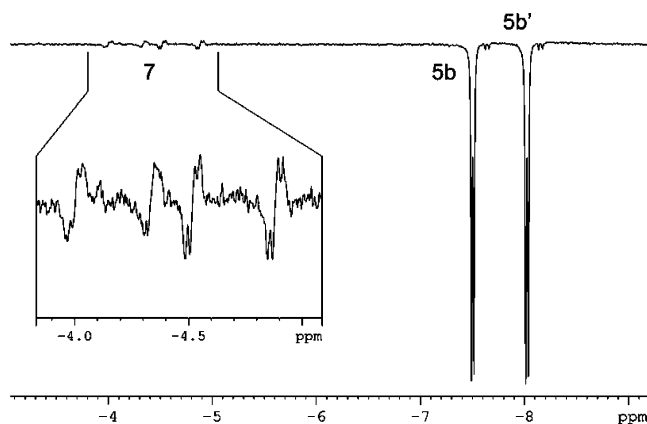


Figure 11. Hydride region of ^1H (upper trace) NMR spectra of the reaction of **1b** with diphenylacetylene- d_{10} , pyridine, and $p\text{-H}_2$ in CD_2Cl_2 at 313 K. The dominant emission signals are for **5b** (right), but those for **5b'** and **7** (expanded inset) can also be seen.

centered at δ –4.21 (ddad, $J_{\text{HH}} = -18.0$ Hz, $J_{\text{HP}} = 138$, 9 Hz) and δ –4.71 (ddad, $J_{\text{HH}} = -18.0$ Hz, $J_{\text{HP}} = 146$, 9 Hz) (where in the multiplicities, “a” = antiphase) (Figure 11). These two proton resonances proved to be coupled to each other and, therefore, must correspond to a dihydride species, which is most likely $[\text{Pd}(\text{t}^{\text{Bu}}\text{cope})(\text{H})_2]$ (**7**). This information indicates that reduction of palladium(II) to palladium(0) is possible under the reaction conditions and provides evidence that a neutral cycle could be entered in CD_2Cl_2 , where we have demonstrated the involvement of species **2**–**5**. It should be noted that complex **7** was only observed in CD_2Cl_2 .

NMR data for complexes **2**–**7** as a function of solvent are summarized in Table 2.

Modified 1D EXSY experiments were then recorded in both solvents to probe magnetization transfer within **2b**. Selective irradiation of the ^1H signals at δ 4.93 and δ 2.91 led to transfer into *trans*-stilbene, while excitation of the δ 3.03 signal revealed exchange into the δ –7.69 signal due to **5b** and the δ 6.63 signal of **4b**. When the δ –7.69 signal was irradiated, transfer into both **4b** and *trans*-stilbene was indicated, although when the signal for **4b** was examined, no chemical activity was evident.

Detection of $[\text{Pd}(\text{t}^{\text{Bu}}\text{cope})(\text{D})(\text{pyridine})](\text{OTf})$. When a sample of **1b** was examined that had been left in methanol- d_4 with ca. 5 equiv of pyridine for 24 h at room temperature, in the absence of hydrogen or the alkyne, a roughly 1:1 mixture of **1b** and a new species, with ^{31}P resonances at positions almost identical to those seen for **5b** in methanol- d_4 , was obtained. The signal at δ –2.45 in the $^{31}\text{P}\{^1\text{H}\}$ spectrum exhibited an extra 1:1:1 triplet splitting of 30 Hz due to an additional coupling to a single *trans* deuterium, which must come from the methanol- d_4 solvent. These two ^{31}P resonances therefore correspond to the deuterated analogue of **5b**, $[\text{Pd}(\text{t}^{\text{Bu}}\text{cope})(\text{D})(\text{pyridine})](\text{OTf})$ (**5b**- ^2H), as shown in Figure 12. As expected, the many-scan 1D proton NMR spectrum showed only a very weak resonance at δ –7.70 for **5b** due to trace amounts of protons in the system. Further proof was obtained when ^{15}N -labeled pyridine was used, since the ^{31}P resonance at δ 101.92 showed the expected extra coupling due to the *trans* pyridine ligand ($J_{\text{PN}} = 26$ Hz).

When this sample was removed from the spectrometer and an excess of diphenylacetylene was added to the solution, the

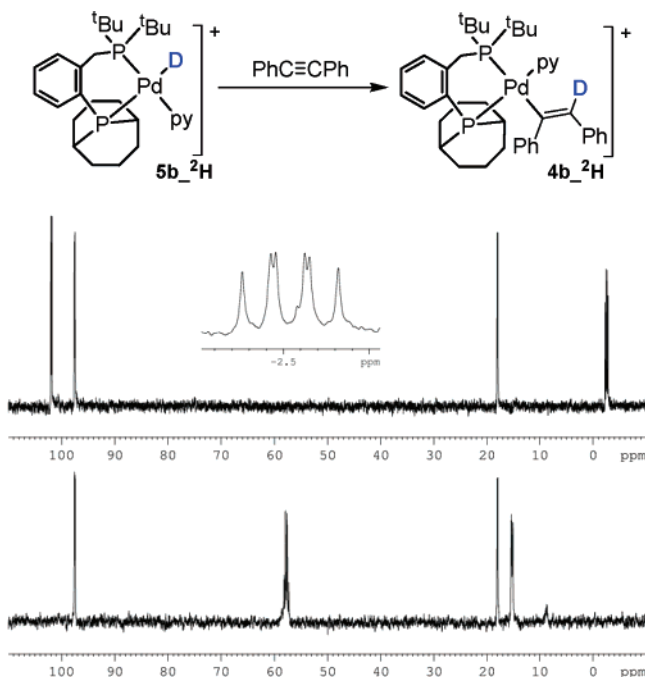


Figure 12. $^{31}\text{P}\{^1\text{H}\}$ NMR spectra of a methanol- d_4 solution of **1b** after 24 h at room temperature (upper trace), showing a ca. 1:1 mixture of the methanol adduct of **1b** [δ_{P} 97.53 (P^{tBu}_2), 17.96 (PC_8H_{14})] and $[\text{Pd}(\text{bucupe})(\text{D})(\text{pyridine})]^+$ (the inset shows the extra *trans* deuterium splitting seen for the $^{31}\text{P}-\text{C}_8\text{H}_{14}$ center); and the same solution after addition of diphenylacetylene (lower trace), indicating the quantitative transformation of $[\text{Pd}(\text{bucupe})(\text{D})(\text{pyridine})]^+$ into **4b**.

new $^{31}\text{P}\{^1\text{H}\}$ NMR spectrum indicated that **5b- ^2H** had been converted into **4b- ^2H** . Not surprisingly, the corresponding ^1H NMR spectrum did not contain a resonance at δ 6.62 due to the vinylic proton of **4b** because the insertion reaction now involved a PdD bond. When this sample was then degassed and charged with 3 atm of *para*-hydrogen, emission signals were seen for the hydride resonance of **5b**, and as well as the vinylic proton of **4b** at δ 6.62 and the three protons of the alkyl cation **2b** showed the PHIP effect. This indicates that $[\text{Pd}(\text{bucupe})(\text{D})(\text{pyridine})](\text{OTf})$ is able to initiate the hydrogenation reaction. Furthermore, GC/MS analysis was also undertaken for the organic components produced from the reaction of preformed $[\text{Pd}(\text{bucupe})(\text{D})(\text{pyridine})](\text{OTf})$ with H_2 and a 3-fold excess of protio-diphenylacetylene (based on the original amount of **1b**). Evidence for complete conversion into *trans*-stilbene was obtained after a reaction time of 5 min, and the ratio of D_0 to D_1 isotopomers of *trans*-stilbene proved to be approximately 2:1. This information confirms that **5b- ^2H** is catalytically active and that H_2 addition leads to the generation of protio-**5b** rather than **5b- ^2H** after **5b- ^2H** is turned over.

Quantitative Magnetization Transfer Studies on 2a and 2b. In order to explore the reactivity of **2a** and **2b** in more detail, a series of 1D EXSY experiments were recorded where the alkyl proton α to the metal was selected, and magnetization transfer from this site was monitored as a function of reaction time. We have already indicated that, when **2a** was examined in this way in CD_2Cl_2 , strong magnetization transfer into the *trans*-stilbene signal at δ 7.18 was observed. This process has been followed as a function of reaction temperature for **2a** in several solvent systems: CD_2Cl_2 , methanol- d_4 , CD_2Cl_2 containing 10% methanol, and both CD_2Cl_2 and methanol- d_4 containing 2 μL of pyridine. **2b** was examined in a similar way using CD_2Cl_2 ,

Table 4. Rate Constants, Activation Parameters ΔH^\ddagger (kJ mol^{-1}) and ΔS^\ddagger ($\text{J mol}^{-1} \text{K}^{-1}$), and Free Energy of Activation ΔG^\ddagger (kJ mol^{-1}) for the Elimination of *trans*-Stilbene from **2a** and **2b** at 300 K

complex	k (s^{-1})	ΔH^\ddagger	ΔS^\ddagger	ΔG^\ddagger_{300}
2a in CD_2Cl_2	0.18	79 ± 7	5 ± 24	77 ± 4
2a in CD_2Cl_2 with 10% methanol	0.21	78 ± 4	3 ± 16	77 ± 1
2a in CD_2Cl_2 + 2 equiv of py	0.27 ^a			77 ^a
2a in methanol- d_4	0.53	42 ± 9	-107 ± 31	75 ± 8
2a in methanol- d_4 + py	0.61	76 ± 1	5 ± 3	75 ± 1
2b in CD_2Cl_2	1.04 ^b	94 ± 6	69 ± 22	73 ± 1

^a Poor data. ^b Extrapolated from Eyring plot.

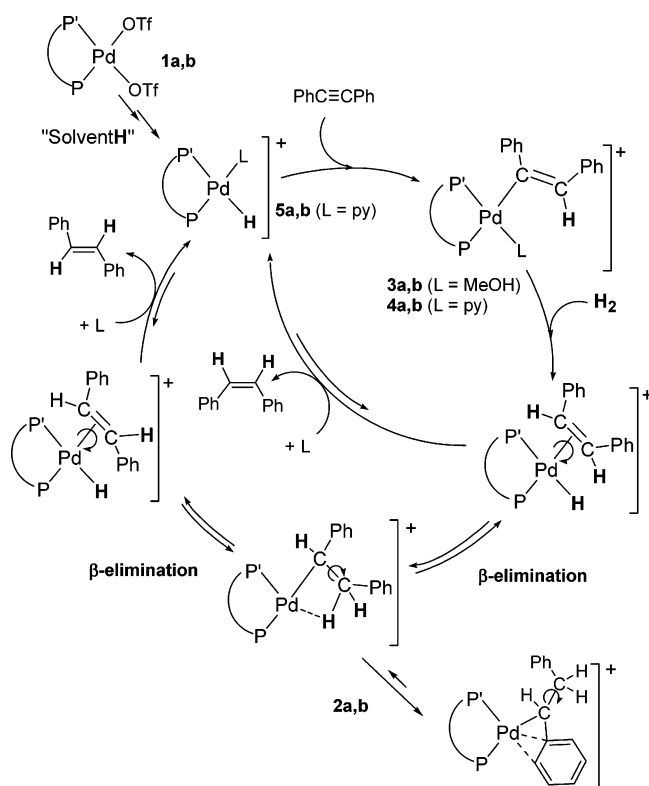
but when methanol- d_4 was used instead, the enhanced signals decayed too fast to record any data. The corresponding observed rates (s^{-1}) for *trans*-stilbene elimination at 300 K, and ΔH^\ddagger , ΔS^\ddagger , and $\Delta G^\ddagger_{(300)}$ values, where obtainable, are presented in Table 4. These data will be discussed in the Conclusions section.

Conclusions

The symmetrical chelating phosphine complex $[\text{Pd}(\text{bcope})(\text{OTf})_2]$ (**1a**), where bcope is $(\text{C}_8\text{H}_{14})\text{PCH}_2-\text{CH}_2\text{P}(\text{C}_8\text{H}_{14})$, and the lower symmetry complex $[\text{Pd}(\text{bucupe})(\text{OTf})_2]$ (**1b**), where 'bucupe is $(\text{C}_8\text{H}_{14})\text{PC}_6\text{H}_4\text{CH}_2\text{P}(\text{tBu})_2$, were prepared and have been shown to catalyze the hydrogenation of diphenylacetylene. In this reaction, *cis*- and *trans*-stilbene and 1,2-diphenylethane are the dominant products.

A number of reaction intermediates have been observed and some kinetic data collected on these two systems that rationalize this behavior. In the first instance, neither **1a** nor **1b** reacts with diphenylacetylene directly in these solvents to produce the three organic products in the absence of hydrogen. However, when methanol- d_4 or CD_2Cl_2 solutions of **1a** or **1b** containing pyridine are examined, the slow formation of the monodeuteride-containing cations $[\text{Pd}(\text{P}_2)(\text{D})(\text{pyridine})](\text{OTf})$ is indicated.⁴⁶ In contrast, when H_2 is added to similar solutions, the formation of the monohydrides $[\text{Pd}(\text{P}_2)(\text{H})(\text{pyridine})](\text{OTf})$ (**5a** and **5b**) occurs, even though methanol- d_4 is present. Examination of the proton signal for free hydrogen reveals that no HD is present after 1 h. This indicates that, under H_2 , **1a** and **1b** can access catalytically active hydride cations of the type that have been proposed for numerous palladium-catalyzed reactions.^{1,51,52}

When the reactions of **1a** and **1b** with diphenylacetylene and *para*-hydrogen in methanol- d_4 or CD_2Cl_2 are examined, the detection of $[\text{Pd}(\text{bcope})(\text{CHPhCH}_2\text{Ph})](\text{OTf})$ (**2a**) and $[\text{Pd}(\text{bucupe})(\text{CHPhCH}_2\text{Ph})](\text{OTf})$ (**2b**) is achieved. In **2b**, the alkyl ligand lies *trans* to the 'tBu-substituted phosphorus center. Crystal structures for the di-aqua complex, $[\text{Pd}(\text{bucupe})(\text{OH}_2)_2](\text{OTf})_2 \cdot 2(\text{H}_2\text{O})$, and the methanol solvate, $[\text{Pd}(\text{bcope})(\text{MeOH})_2](\text{OTf})_2 \cdot 2\text{MeOH}$, illustrate the fact that these cations coordinate effectively to relatively weak donor ligands, and it might be expected that such a situation would be found during catalysis. The spectroscopic signatures of the two alkyl cations do not, however, change with solvent, even when pyridine is added, and to achieve an acceptable 16-electron count, a stabilizing interaction with the arene π system of the alkyl ligand is suggested from our experimental data. The NMR data support an η^3 -benzyl interaction, in accordance with DFT calculations that have revealed a preference for η^3 -benzyl interactions over β -agostic interactions in a related complex.⁵⁵ In addition, a role for related η^3 -benzyl complexes has been demonstrated by

Scheme 4. Schematic Mechanism Showing Alkene Formation and Isomerization

Hartwig et al. in the hydroamination of vinylarenes^{56,57} and by Brown et al. and Brookhart in the Heck reaction.^{8,47,58}

Evidence for β -hydrogen transfer in related palladium bis-phosphine cations containing an alkyl ligand has also been presented by Brown et al. during a study of the Heck reaction.⁵⁹ They suggest that an undetected palladium alkene hydride complex is involved in the liberation of the corresponding alkene.

In the case of **2a** and **2b**, the interaction with the arene π system would need to be broken in order for this to happen. Scheme 4 shows an alternative formulation for species **2**, featuring a β -agostic interaction between one of the β -CH protons of the alkyl ligand and the metal center. The resulting β -hydrogen transfer is likely to involve an intermediate with a β -agostic interaction, and intermediates of this type have been shown to play a direct role in related reactions (i.e., ethylene polymerization).⁵¹

Both **2a** and **2b** have, in fact, been shown by EXSY to play a direct role in the formation of the two semihydrogenation products. When magnetization transfer from the α -H of the CHPhCH_2Ph is monitored, the formation of *trans*-stilbene is indicated as the major pathway, although limited exchange into the other two sites is also seen. The two β -H's of the alkyl cations are distinct, with magnetization transfer from one proceeding into *trans*-stilbene and from the other into a number of distinct sites that depend explicitly on the solvent.

In CD_2Cl_2 , transfer is observed from the δ 3.13 site of **2a** into both *cis*-stilbene and H_2 . In contrast, when the analogous process is monitored in methanol- d_4 , magnetization proceeds from the δ 3.13 site into the vinyl proton of **3a**, $[\text{Pd}(\text{bcope})-(\text{CPh}=\text{CHPh})(\text{methanol})](\text{OTf})$. The process by which this interconversion occurs was identified by the addition of pyridine, since magnetization transfer from this site proceeds into $[\text{Pd}(\text{bcope})(\text{CPh}=\text{CHPh})(\text{pyridine})](\text{OTf})$ (**4a**), the pyridine-solvated monohydride $[\text{Pd}(\text{bcope})(\text{H})(\text{pyridine})](\text{OTf})$ (**5a**), and the related species $[\text{Pd}(\text{H})(\text{bcope})(\eta^1\text{-bcope})](\text{OTf})$ (**6**); when free bcope is added, magnetization transfer from this site proceeds only into **6**. This confirms that the β -H of the CHPhCH_2Ph group of **2a**, which resonates at δ 3.13, actually transfers first into $[\text{Pd}(\text{bcope})(\text{H})(\text{L})](\text{OTf})$, where L = methanol or pyridine, and then into $[\text{Pd}(\text{bcope})(\text{CPh}=\text{CHPh})(\text{L})](\text{OTf})$ via reaction with a fresh molecule of diphenylacetylene. At the same time that this occurs, *trans*-stilbene is eliminated from **2a**. It proved possible to demonstrate a role for **5a** in this process directly by showing that magnetization transfer from the hydride site of **5a** proceeds directly into both the vinyl proton site of **4a** and *trans*-stilbene.

When the corresponding process was examined for **2b**, magnetization transfer into *trans*-stilbene was again observed from two sites of the alkyl, while transfer into either hydride species **5b** or **5b'**, or the vinyl complexes **3b** and **4b**, was seen, depending on whether the pyridine was present or not. These deductions are summarized in Scheme 4.

It is worth noting at this stage that, remarkably, the single vinylic CH protons in **3** and **4** and the single hydride ligand in **5** appear as strong emission signals in the corresponding ^1H NMR experiments. This is an example of one-proton PHIP and illustrates the care with which $p\text{-H}_2$ experiments need to be examined if the correct deductions are to be made, since species such as $[\text{Pd}(\text{P}_2)(\text{cis-stilbene})]$ or $[\text{Pd}(\text{P}_2)(\text{H})_2(\text{pyridine})]$ might otherwise be invoked. Magnetization transfer experiments indicated that the kinetic fate of **3** and **4** could not be determined because they were unreactive on the NMR time scale.

Nonetheless, these species are not stable under these conditions and must be involved in the formation of the hydrogenation products on a longer time scale. The addition of H_2 in a slow step to **2**, the alkyl cation, is necessary if the formation of H_4 -labeled 1,2-diphenylethane in methanol- d_4 is to be explained.

For the $^t\text{bcope}$ system, single isomers of both $[\text{Pd}(^t\text{bcope})-(\text{CHPhCH}_2\text{Ph})](\text{OTf})$ (**2b**) and $[\text{Pd}(^t\text{bcope})(\text{CPh}=\text{CHPh})(\text{pyridine})](\text{OTf})$ (**4b**) were seen, while two isomers of $[\text{Pd}(^t\text{bcope})(\text{H})(\text{pyridine})](\text{OTf})$ (**5b** and **5b'**) were detected. In **2b**, the alkyl arm is *trans* to the ^tBu -bearing phosphorus center, and the vinyl group is arranged in a similar way in **4b**, but the opposite is true for the hydride orientation in **5b**, where it is *trans* to the cope-bearing phosphorus center. This information is summarized in Chart 2 and Scheme 4. β -H transfer in **2b** locates the new hydride ligand *trans* to the cope-bearing phosphorus arm, and loss of alkene and binding of pyridine then lead directly to **5b**, while binding of the alkyne leads to **4b** if the hydride ligand moves onto one of the unsaturated alkyne carbons.

It should also be noted that, when the symmetry-breaking phosphine $^t\text{bcope}$ is employed, enhanced hydride signals are also seen for the dihydride complex $[\text{Pd}(^t\text{bcope})(\text{H})_2]$ (**7**). This

(55) Ludwig, M.; Strömberg, S.; Svensson, M.; Åkermark, B. *Organometallics* **1999**, *18*, 970–975.

(56) Nettekoven, U.; Hartwig, J. F. *J. Am. Chem. Soc.* **2002**, *124*, 1166–1167.

(57) Johns, A. M.; Utsunomiya, M.; Incarvito, C. D.; Hartwig, J. F. *J. Am. Chem. Soc.* **2006**, *128*, 1828–1839.

(58) Rix, F. C.; Brookhart, M.; White, P. S. *J. Am. Chem. Soc.* **1996**, *118*, 2436–2448.

(59) Brown, J. M.; Hii, K. K. M. *Angew. Chem., Int. Ed. Engl.* **1996**, *35*, 657–659.

means that, when CD_2Cl_2 is the reaction medium, the formation of a Pd(0), Pd(II) reaction cycle involving neutral species is possible.

This reaction proved to be solvent-dependent, with methanol leading to higher activities than CD_2Cl_2 for both **1a** and **1b**, although **1b** shows a higher overall activity than **1a** for the consumption of diphenylacetylene. This is reflected in the higher first-order rate constants for the production of *trans*-stilbene that were measured for the bcope system in methanol- d_4 , as illustrated in Table 4. The product distribution is critically dependent on the phosphine, with the bcope system forming substantial amounts of the double hydrogenation product 1,2-diphenylethane when compared to the 'bucope system (25% rather than <1% when the complete conversion of diphenylacetylene is achieved). Furthermore, the bcope system also produces more of the dimerization product *E,E*-1,2,3,4-tetraphenylbuta-1,3-diene than the 'bucope-based catalyst, although the level of conversion, at 1%, means that it is not formed in a significant reaction pathway.

We also know that **1a** and **1b** are stable indefinitely in CD_2Cl_2 , and in methanol we were successful at crystallizing **1a**·MeOH. In contrast, while **1b** was stable in methanol, it reacted in methanol- d_4 containing pyridine to form the mono-deuteride **5b-²H**. We therefore believe that the greater activity seen in methanol results from the improved efficiency of catalyst conversion into active species in this solvent.

For **2a**, the elimination of *trans*-stilbene proceeds in methanol- d_4 at a rate of 0.53 s^{-1} at 300 K, where $\Delta H^\ddagger = 42 \pm 9 \text{ kJ mol}^{-1}$ and $\Delta S^\ddagger = -107 \pm 31 \text{ J mol}^{-1} \text{ K}^{-1}$. When the corresponding reaction is completed in CD_2Cl_2 , the corresponding rate constant falls to 0.18 s^{-1} , while ΔH^\ddagger becomes $79 \pm 7 \text{ kJ mol}^{-1}$ and ΔS^\ddagger becomes $5 \pm 24 \text{ J mol}^{-1} \text{ K}^{-1}$. The analogous process for **2b** proved to be too fast to monitor accurately in methanol, but when CD_2Cl_2 was employed, the corresponding rate constant for *trans*-stilbene formation is 1.04 s^{-1} at 300 K, with $\Delta H^\ddagger = 94 \pm 6 \text{ kJ mol}^{-1}$ and $\Delta S^\ddagger = 69 \pm 22 \text{ J mol}^{-1} \text{ K}^{-1}$. These data match those obtained from the product studies, where **2b** proved faster and produced the largest amounts of *trans*-stilbene.

The activation entropy for alkene liberation for **2a** in CD_2Cl_2 is $-5 \pm 24 \text{ J mol}^{-1} \text{ K}^{-1}$, which suggests that solvation effects are relatively limited. As a consequence, the enthalpy of activation is relatively high, at $79 \pm 7 \text{ kJ mol}^{-1}$. Upon changing the solvent to methanol, the activation entropy for alkene liberation for **2a** falls to $-107 \pm 31 \text{ J mol}^{-1} \text{ K}^{-1}$, which suggests that solvation effects become much more important, in accordance with the fact that methanol- d_4 is a better donor than CD_2Cl_2 . This deduction is matched by the lowering of the enthalpy of activation to $42 \pm 9 \text{ kJ mol}^{-1}$ in methanol- d_4 .

It is also important to note that GC/MS analysis of the organic products produced in these reactions revealed proton rather than deuterium incorporation for reactions involving H_2 in methanol- d_4 until **5b-²H** was used as the catalyst precursor. This situation changed when **5b-²H** was used as the catalyst precursor because evidence for ²H incorporation into the *cis*-stilbene was observed. We therefore conclude that the active palladium hydrides are recycled, as shown in Scheme 4, via reactions involving H_2 rather than methanol- d_4 . The initial formation of **5** via oxidation of the solvent rather than H_2 addition cannot, however, be ruled out.^{2,10}

The product distribution seems to be related to the lifetime of the alkyl cation, which is longest for **2a**, where substantial amounts of 1,2-diphenylethane are obtained in a reaction which involves H_2 addition to **2**. The binding of diphenylacetylene to either **3** or **4**, followed by C–C bond formation and the addition of H_2 , is necessary to account for the formation of *E,E*-1,2,3,4-tetraphenylbuta-1,3-diene.

Acknowledgment. We are grateful for EU funding under the HYDROCHEM network (contract HPRN-CT-2002-00176). We are also grateful to Prof. Paul Pringle (University of Bristol) for the bcope and 'bucope ligands and to Prof. Robin N. Perutz (University of York) for helpful discussions.

Supporting Information Available: X-ray tables and some synthetic details (PDF, CIF). This material is available free of charge via the Internet at <http://pubs.acs.org>.

JA070331C